Trace and minor elements in sphalerite: an assessment of distributions in metamorphosed deposits:

Thesis submitted in accordance with the requirements of the University of Adelaide for an Honours Degree in Geology

Julian Anthony Lockington

November 2012

TRACE AND MINOR ELEMENTS IN SPHALERITE: AN ASSESSMENT OF DISTRIBUTIONS IN METAMORPHOSED DEPOSITS:

ABSTRACT:

Sphalerite is a common sulphide mineral and occurs in ore deposits of various types. It is the major ore mineral in the majority of Zn-Pb sulphide deposits. The emergence of precise, high-resolution microanalytical methods, such as Laser-Ablation Inductively-Coupled-Plasma Mass-Spectrometry (LA-ICP-MS) has allowed for greater precision in the analysis of the minor and trace elemental characteristics of sulphides, including sphalerite. These methods have evolved to become valuable petrogenetic tools over the past decade. In this study Laser-Ablation Inductively-Coupled-Plasma Mass-Spectrometry (LA-ICP-MS) has been used to analyse 19 sulphide samples from metamorphosed sphalerite-bearing deposits in Norway and Australia. The distributions of Mn, Fe, Co, Cu, Ga, Se, Ag, Cd, In, Sn, Sb, Hg, Tl, Pb and Bi have been investigated with particular attention to how concentrations of these elements vary with metamorphic grade and the extend of sulphide recrystallisation and syn-metamorphic deformation. The study has also attempted to address any possible correlations among the different elements. The results were found to indicate that trace elements which are believed to exist as micro- to nano-scale inclusions in sphalerite (such as Cu, Pb and Bi) are reduced in abundance with increasing metamorphic grade. This is due to recrystallisation resulting in these small scale inclusions being removed from the sphalerite and remobilised to form discrete minerals elsewhere. The distributions of lattice-bound elements (Mn, Fe, Cd, In, Hg) show few trends, suggesting that source and physico-chemical conditions of primary crystallisation are dominant in defining the concentrations of these elements. A moderately strong positive correlation between copper and indium concentrations was also identified, confirming previously published data.

KEY WORDS

Sphalerite, metamorphism, trace, elements, distribution, mass spectrometry, laser ablation

Table of contents:

LIST OF FIGURES AND TABLES

Trace and minor elements in sphalerite

INTRODUCTION:

Zinc sulphide (ZnS) occur naturally in three forms, sphalerite, wurtzite and matraite. Of these, sphalerite, made up of Zn and S atoms arranged in a tetrahedral coordination within a face-centred cubic lattice, is by far the most common form. Sphalerite and wurtzite can often occur as intergrown crystals down to the sub-micron scale and can even occur together in columnar aggregates in some sulphide deposits (Minceva-Stefanova 1993). Because of this it can be difficult to distinguish with certainty whether a sphalerite grain may contain some nanolayers of wurtzite.

Sphalerite is the main ore for zinc and is the dominant mineral in most zinc sulphide deposits. Such sulphide deposits can occur in a variety of genetic types such as epithermal vein deposits, skarns, volcanogenic massive sulphide (VMS) deposits, stratabound sedimentary exhalative (SEDEX) deposits and Mississippi-Valley-Type (MTV) deposits.

Sphalerite is capable of incorporating a wide range of minor and/or trace elements, sometimes in concentrations that are economic to extract (such as in the case of germanium or indium) or pose environmental and/or processing problems in the case of unwanted elements (such as cadmium or manganese) (Cook *et al.* 2009). Cadmium is of particular interest since it can occur at high enough concentrations for it to become economic to exploit as a by product, but is otherwise an unwanted contaminate.

As well as potentially effecting the economic value of zinc sulphide deposits, the distribution of minor and trace elements in sphalerite can be an important source of

petrographic information, especially in terms of identifying the genetic type and source fluid of the sulphide deposit (Cook *et al.* 2009; Lin *et al.* 2011). These studies have also investigated potential relationships between the concentrations of certain elements, for example, whether relatively high concentrations of one element correlates with an increase or decrease in concentrations of another element or whether the distributions of minor and trace elements within sphalerite correlates with the geologic history of the deposits they are contained in.

The published literature on sphalerite geochemistry shows that that cobalt and indium tend to be concentrated in relatively high temperature hypothermal and mesothermal ore deposits while anomalous gallium, germanium, mercury and tin tend to be found in higher concentrations in lower temperature epithermal ores. Furthermore it has been suggested that germanium-rich sphalerite tends to have a lower formation temperature than indium-rich sphalerite (Logan 2004, Cook *et al.* 2009, Lin *et al.* 2011)

While the effects that regional metamorphism of a sulphide deposit can have on sulphides such as pyrite, chalcopyrite and pyrrhotite have been studied before in papers such as Larocque & Hodgson (1995) and Large *et al.* (2009), the effects of regional metamorphism on sphalerite has not been investigated in such detail. The deposits analysed in this study cover a range of metamorphic conditions ranging from low to high grade, and by comparing the elemental distributions between different deposits the effects of regional metamorphism will be identified.

Trace and minor elements in sphalerite

Some older published studies reporting unusually high concentrations of a wide range of minor and trace elements have been at least partially disproved with the advent of electron beam analysis techniques replacing older "wet chemistry" analysis techniques. Electron beam techniques were able to show that in some cases that the measured high trace element concentrations were caused by micro scale inclusions of other minerals which contained the supposed trace elements instead of the elements occurring at high concentrations in the sphalerite lattice (Cook *et al.* 2009). However the electron microprobe cannot provide the necessary precision to accurately measure elemental concentrations down to the sub-ppm level.

Studies such as Reed (1990), Jackson *et al.* (1992), Perkins *et al.* (1993), Fryer *et al.* (1995), Watling *et al.* (1995) and others demonstrated that modern analytical techniques such as Laser Ablation-Inductively Coupled Plasma Mass Spectrometry (LA-ICPMS) can be applied to accurately determine the nature and trace element composition of minerals. This technique can complement electron microprobe analysis in the characterisation of minerals.

The advantages of LA-ICPMS include much lower detection limits, the ability to, in some cases, provide direct or indirect information as to whether the trace element in question is located within the sphalerite crystal lattice or in nano to micro-scale inclusions, and the capability of analysing a greater volume of material which allows for the biasing effect of inhomogeneities to be smoothed out (Cook *et al.* 2009). Trace element distributions in sulphides can now be analysed accurately and efficiently using LA-ICPMS since suitable standards are available. The method allows trace element

analysis of sulphides in general (Watling *et al.* 1995; Danyushevsky *et al.* 2012), and sphalerite in particular (Axelsson & Rodushkin 2001; Cook *et al.* 2009) to be carried out with confidence.

Whereas the development of electron beam analysis techniques has allowed for increased accuracy regarding the distributions of elements within zinc sulphides, uncertainties about the real range of minor and trace element concentrations within the sphalerite lattice itself persist. This is due to it not always being possible to discriminate between elements hosted within the sphalerite crystal lattice and elements hosted within sub-micron and nanoscale inclusions, especially in sphalerite from fine grained ores, even at the scales of the electron microprobe beam (Cook *et al.* 2009).

GEOLOGICAL SETTINGS OF THE DEPOSITS:

This study is based on the analysis of ZnS samples taken from various Norwegian and Australian zinc sulphide deposits. This data will be compared with previously published data for zinc sulphides from around the world.

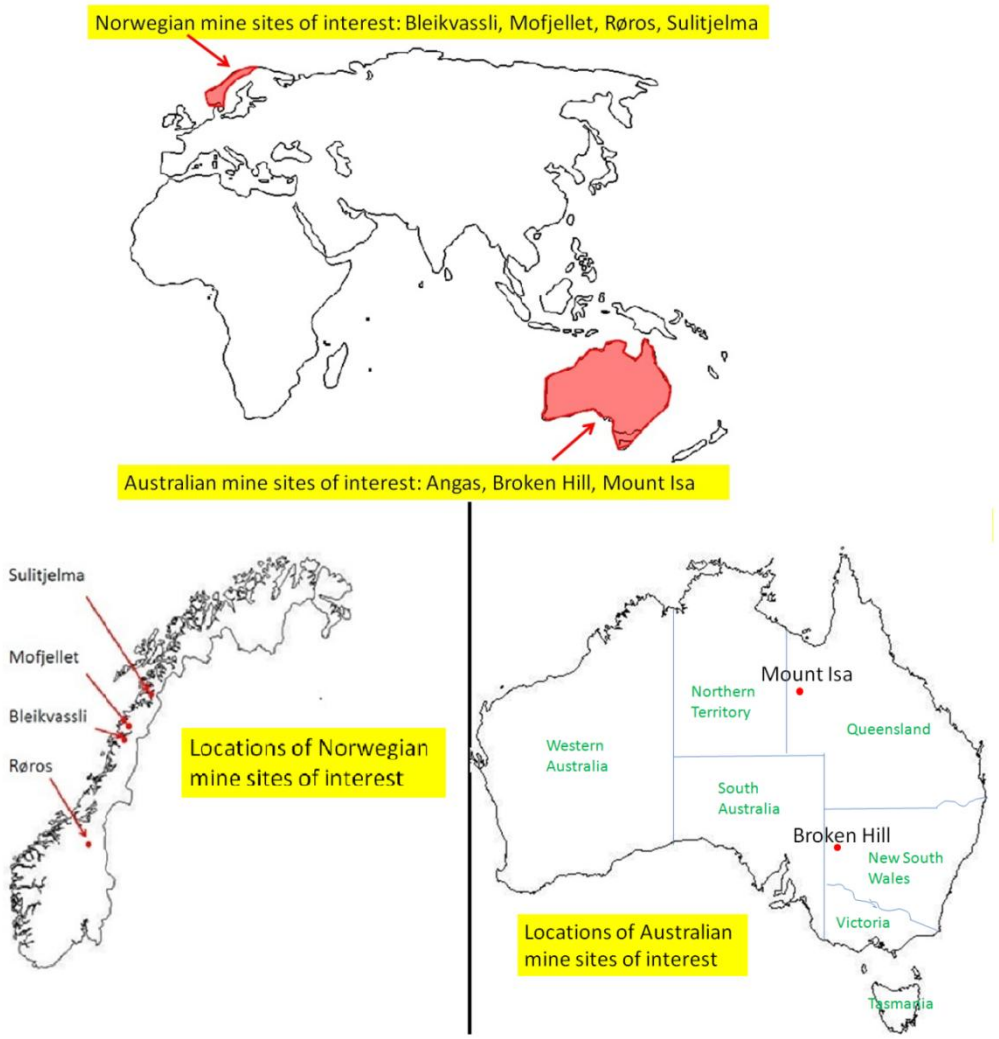

Figure 1: Sketch maps showing the locations of the sites from which the rock samples analysed in this study were taken from. Figure comprises nation outlines from About.com, 2012. <http://geography.about.com/library/blank> The New York Times Company. Website last visited 17/05/2012, and world outline from Outline world map images, <www.outline-world-map.com> Website last visited 17/05/2012, which were altered to display location using information from Barrie et al. (2010a), Barrie et al. (2010b), Haydon & McConachy (1987), Swager (1985) and Terramin (2012).

The Norwegian samples that are to be investigated in this study are from deposits in Bleikvassli, Mofjellet, Røros and Sulitjelma. These deposits are all of VMS or SEDEX type (Barrie *et al.* 2010a) and were significant base metal mines until the late 1980's. The Australian samples are sourced from Broken Hill (New South Wales) and from Mt. Isa (Queensland).

Country	Deposit	Genetic Type	Metamorphic Type	Samples	References
Australia	Mt. Isa	SEDEX	Greenschist facies	5984A 5984B	Large *et al.* 2005
Norway	Røros	VMS	Greenschist to lower amphibolite facies	STO-175-04 STO-175-05 STO-175-06	Grenne *et al.* 1999
Norway	Sulitjelma	VMS	Amphibolite facies	NC5835 NC6005 Sulis 1b Sulis 2a Sulis 2b	Cook 1996
Norway	Mofjellet	SEDEX	Amphibolite facies	Mo2 Mo5 Mo10	Grenne *et al.* 1999
Norway	Bleikvassli	SEDEX	Upper amphibolite to lower granulite facies	Bv1 V59.197 V60.446 V61.538	Cook 1993 Moralev *et al.* 1995 Rosenberg *et al.* 1998
Australia	Broken Hill	SEDEX	Upper granulite facies some retrograde	BH218 BH221	Binns 1964 Corbett & Phillips 1981 Haydon & McConachy 1987

Table 1: summary of the deposits analysed in this study.

The Norwegian samples all come from the Scandinavian Caledonides, a belt of late Precambrian to early Palaeozoic rocks which have been variably deformed and metamorphosed during the Caledonian Orogeny, they presently exist as a series of nappes and thrust sheets (Grenne *et al.* 1999; Barrie *et al.* 2010a).

The Sulitjelma deposit is located near the town of Sulitjelma in northern Norway, over 20 massive sulphide orebodies have been found, located at the contact between a dominantly basaltic sequence called the Otervatn Volcanic Formation and a thick overlying sedimentary unit called the Furulund Group (Cook *et al.* 1990). The Sulitjelma orebodies are believed to have formed during a single stratigraphic interval during the Ordovician as a result of intense hydrothermal alteration of seafloor basaltic rocks together with chemical exhalative precipitation from the hydrothermal fluids as

they emerged into the ocean water of the sea floor (Cook *et al.* 1990), much like what can be seen occurring at so called "black smoker" hydrothermal vents at places on the sea floor in the present day. Post formation the deposit experienced amphibolite facies metamorphism and was significantly deformed (Cook *et al.* 1993; Cook 1996).

The Bleikvassli deposit is located roughly 46 km southeast of the city of Mo i Rana, it is hosted within amphibolites, quartzites, mica schists and quartzofeldspathic gneisses and has a main orebody made up of interlayered lenses of massive sulphide ore. The deposit is believed by most researchers to be of SEDEX origin (Cook 1993; Moralev *et al.* 1995; Rosenberg *et al.* 1998) due to being hosted in a dominantly sedimentary succession. The deposit has been metamorphosed after formation with peak temperature of roughly 570 ^{O}C and pressure of 7.5 to 8 kilobars, lying within an area of highly deformed mica schist rock (Cook 1993; Rosenberg *et al.* 1998).

The Mofjellet deposit, located roughly 1 kilometre south of the city of Mo i Rana, is hosted within gneissic rocks from the Mofjellet Group in the Rødjngsfjellet Nappe complex (Grenne *et al.* 1999; Bjerkgård *et al.* 2001) . Like Bleikvassli this deposit appears to be of SEDEX origin type and is generally layered and semi-massive instead of massive.

The Røros region is a polymetallic orefield located in the Trondheim region of the Caledonides, the deposits there are hosted within a Cambrian to Silurian succession of turbidites which formed on the sea floor (Barrie *et al.* 2010b).

The Broken Hill ore body lies within the Broken Hill block, within the Willyama Supergroup (Haydon & McConachy 1987). The Broken Hill block is made up of early to middle Proterozoic rocks which encompass a range of metamorphic lithologies including pelitic, quartzofeldspathic and mafic rocks (Pidgeon 1967; Haydon & McConachy 1987). There is a regional progressive increase in metamorphic grade going from the northwest to the southeast of the region, ranging from andalusite grade to granulite grade (Binns 1964). Strong evidence for retrograde metamorphism having influenced the Broken Hill block during late stage deformation exists (Corbett & Phillips 1981). This deposit has experienced very high temperature metamorphism and has extensively recrystallised. Some researchers (Frost *et al.* 2002, 2005) have argued that extensive melting of the sulphide assemblages may have occurred. Others (eg, Spry *et al.* 2008) suggest that although there may have been localised partial melting of minor parts of the ore, there was no substantial liquidation of the sulphides.

The Mt Isa ore body lies within the Mt Isa Inlier, which is a multiply deformed terrain in which basement rocks are overlain by thick successions of volcanic and sedimentary rocks (Page & Sweet 1998). The Mt Isa Inlier is part of a larger Mt Isa-McArthur basin system which contains many major sulphide deposits (Large *et al.* 2005). Located within the Urquhart Shale, which is a middle Proterozoic aged sedimentary unit which is part of the larger Mount Isa Group, the stratiform orebodies of Mt Isa are hosted within carbonaceous and pyritic dolomitic sections of the Urquhart Shale, which has experienced low grade metamorphism but has experienced at least three phases of deformation (Swager 1985). Classified as a SEDEX deposits like the other deposits in

the Mt Isa-McArthur basin, the Mt Isa ore body has experienced greenschist facies metamorphism (Large *et al.* 2005).

METHODS:

Sample selection:

A total of 19 rock samples were investigated. 15 of these samples were from sulphide deposits from Norway while the remaining 4 were taken from sulphide deposits in Australia.

The Norwegian samples were collected by Nigel Cook during the period 1985-2002 for studies on each of four deposits, Sulitjelma (Cook *et al.* 1990; Cook *et al.* 1993; Cook 1994), Bleikvassli (Cook 1993; Cook *et al.* 1998), Mofjellet (Cook 2001) and the Røros orefield (Barrie *et al.* 2010a).

The Australian samples derive from the University of Adelaide Geology and Geophysics teaching collection. Precise locations of these samples within the Broken Hill and Mt. Isa deposits are unknown.

Analytical methodology

Three analytical techniques were used to analyse the sulphide samples, optical microscopy (OM), scanning electron microscopy (SEM), and laser ablation inductively

coupled plasma mass spectrometry (LA ICP MS). All three instruments were located within Adelaide Microscopy, Adelaide University.

Optical Microscopy (OM):

A Nikon petrological microscope with a magnification of up to 50x was used to take reflected light images of the samples. This was used together with SEM to identify and characterise the general texture of the samples, as well as grain relationships and possible overprinting features.

Scanning Electron Microscopy (SEM):

SEM was carried out using a Philips XL30 Field Emission Scanning Electron Microscope. It was equipped with an energy dispersive X-ray spectrometer (EDAX) and a back scattered electron (BSE) detector. The SEM was set at an accelerating voltage of 20keV and a spot size of 4. The BSE detector allows for any compositional zoning present within individual grains to be identified. The EDAX was used for identifying the approximate major elemental composition of mineral grains, allowing for the type of mineral to be identified. However it was not judged accurate enough to be used for trace and minor element distribution measurement, for which LA-ICP-MS was used instead.

Laser Ablation Inductively Coupled Plasma Mass Spectrometry (LA ICP MS):

The LA-ICP-MS was carried out using a UP-213 NdYag New Wave pulsed solid state laser, coupled to an Agilent 7500cx ICP Quadrupole Mass Spectrometer. Glitter software was used for data reduction.

Trace and minor elements in sphalerite

Suitable zinc sulphide grains of interest within the samples were ablated, having been previously identified during the OM and/or SEM analysis of the samples. Analyses were made using a spot diameter of 30μm, with the laser operating at 5Hz pulse rate and 80% power level. Measured isotopes were ^{23}Na, ^{29}Si, ^{33}S, ^{34}S, ^{43}Ca, ^{51}V, ^{52}Cr, ^{55}Mn, ^{57}Fe, ^{59}Co, ^{60}Ni, ^{65}Cu, ^{66}Zn, ^{69}Ga, ^{75}As, ^{82}Se, ^{95}Mo, ^{107}Ag, ^{111}Cd, ^{115}In, ^{118}Sn, ^{121}Sb, ^{125}Te, ^{137}Ba, ^{184}W, ^{193}Ir, ^{197}Au, ^{202}Hg, ^{205}Tl, ^{208}Pb and ^{209}Bi. An analysis time of 90 seconds was used, with 30 seconds spent measuring background levels with the laser off and 60 seconds spent measuring the ablated material with the laser on. Data reduction was undertaken using Zn as the internal standard for the zinc sulphides.

Calibration was done by using the MASS-1 (formerly known as PS-1) trace element standard developed for use as a sulphide standard material (Wilson *et al.* 2002). Multiple standard analyses were run at the beginning and end of each period of sampling so that possible instrument drift could be checked for.

RESULTS:

Petrographic pictures

Preceding the analytical work, each sample was investigated by optical microscope and SEM. Photomicrographs and back-scatter electron images were taken to illustrate each sample.

The 19 samples analysed came from deposits ranging in metamorphic grade from greenschist facies (Mt Isa) to upper granulite facies (Broken Hill). As such the texture

and mineral natures of the samples varied significantly between samples from different deposits. One of the things which did not differ between the samples from the various deposits is that the sphalerite in all of the samples showed no signs of compositional zoning (See Figure 8)

Mt. Isa (samples 5984A and 5984B)

While mostly coarse-grained samples were deliberately chosen for analysis in this study, the samples from Mt. Isa were much finer-grained than those from the other deposits (Figure 2). The Mt Isa samples displayed a series of light and dark, mm- to cm-scale banding, similar in shape at low magnification to the luecosomes and melanosomes that might be found in rocks of much higher metamorphic grade. The grain size of the samples are, however, much finer than would be expected of a high-grade metamorphic rock. As well as light and dark coloured bands being seen throughout the samples, bands of finer and coarser grain size can also be observed. Despite this, and as Figure 2 A, C, E and F show, there is no apparent relationship between the colouration of the bands and the grain size, with both light and dark bands occurring as both finer and coarser grained bands in different parts of the samples.

Clear evidence of overprinting is seen in Figure 2 C. Here, a pyrite grain which is unusually coarse and euhedral (cubic) compared to most of the pyrites in the samples can be seen to have been partially overprinted by later sphalerite and quartz. Apart from a few unusually large and angular pyrite grains seen sporadically throughout the samples, the mineral grains are mostly amorphous in shape. This may indicate that any recystallisation, if it occurred at all during one or more overprinting events, involved the

breakdown of crystal grain edges instead of crystal grain growth, possibly indicating some form of retrograde metamorphism may have occurred, the banding (both in colour and in grain size) may indicate some form of deformation linked retrograde metamorphism acting through small scale shear zones, or may simply be a result of preserved syn-sedimentary banding.

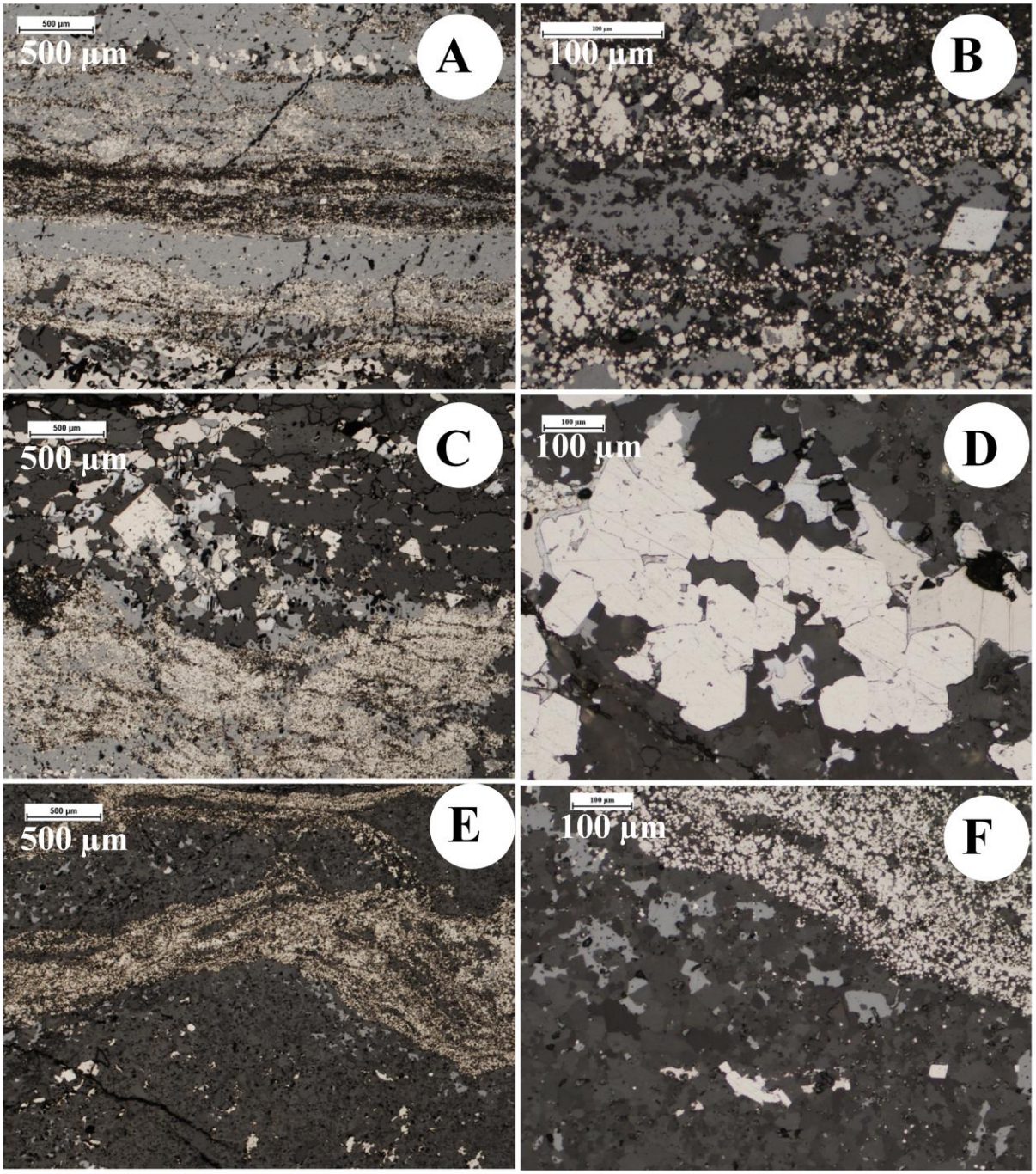

Figure 2: Photomicrographs in reflected light of the two samples from Mt. Isa. (A) shows the general pattern of light and dark bands which pervade the samples. (B) is a close-up of the centre of the picture shown in (A) and shows the amorphous grain shapes of the fine grained minerals. (C) shows a contrast between a fine-grained band and a coarser band and, together with (D) shows that while some of the larger mineral grains show polyhedral shapes, most occur as amorphous grains. (E) shows an example of a band bending. (F) shows the contact between a light and a dark band up close.

Røros (STO-175-04, STO-175-05, STO-175-06)

Unlike the Mt Isa samples, the mineral grains in the samples from Røros are consistently coarse-grained, apart from some fine grained inclusions in larger grains. No overall structural features were observed. Possible signs of overprinting of the sphalerite and/or pyrrhotite by quartz were observed, as shown in Figure 3 E. One of the most striking observable features of the samples was the high abundance of the pyrrhotite (with strong reflectance pleochroism) found within the samples, as shown by Figure 3 C and D. Like Mt Isa, the mineral grains in these samples were amorphous in shape, seemingly 'flowing' into each other in places (Figure 3 A, E and F). The lack of straight edges in the grains of these samples possibly indicate the presence of overprinting after formation, Figure 3 E especially seems to show signs of quartz overprinting of sphalerite.

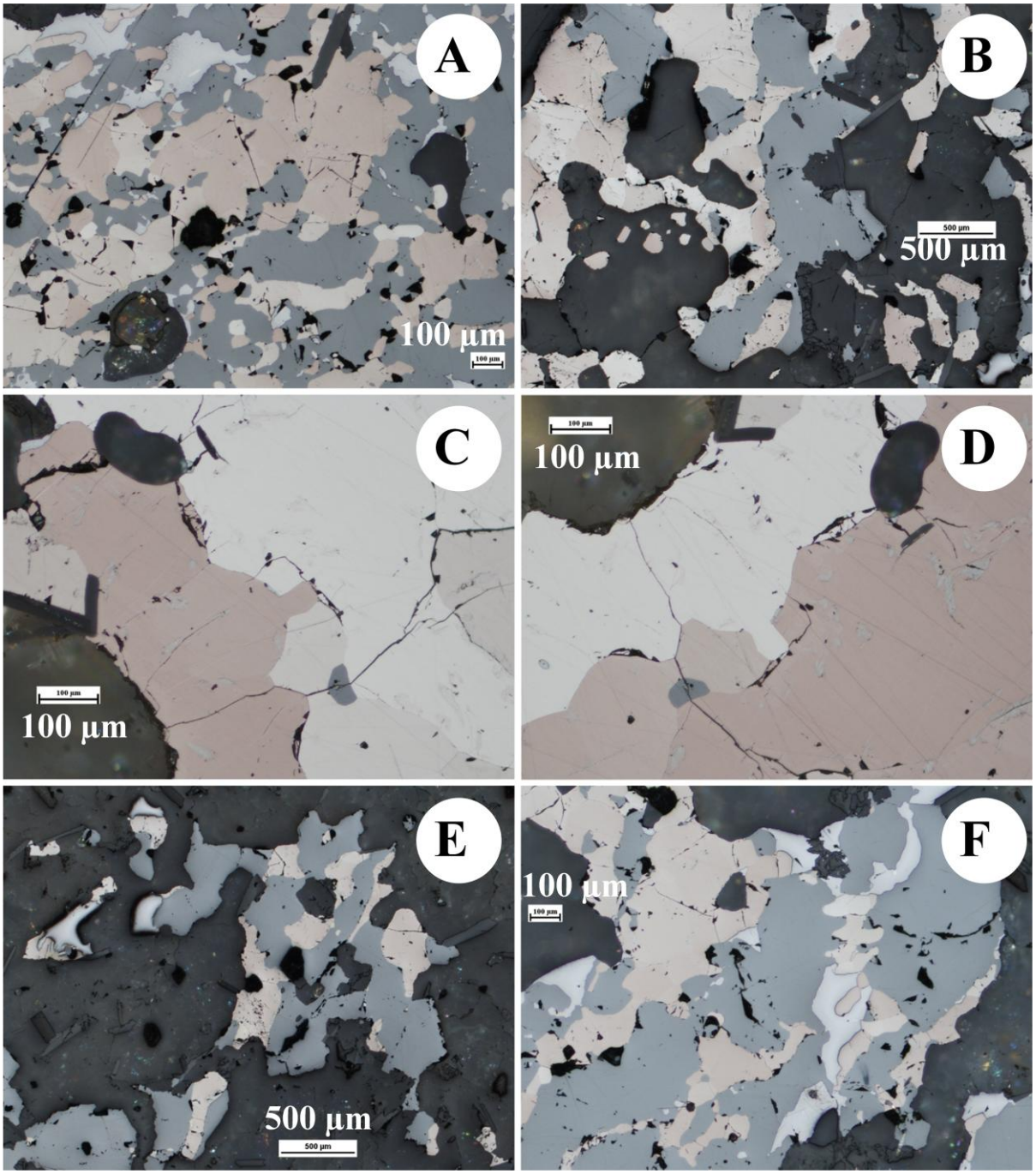

Figure 3: Photomicrographs in reflected light of the samples from Røros. (A) and (B) show the general texture of most of the samples, with course yet amorphous grains pervading throughout. (C) and (D) show the strongly pleochroic pyrrhotite grains in the samples, ranging in colour from white to a deep pink depending on the angle at which they are viewed. (E) and (F) show the general nature of the sphalerite in the samples, with the sphalerite, pyrrhotite and galena mixing together and occurring as inclusions in each other. Also of note is that (E) appears to show quartz overprinting of the sphalerite occurring in some places.

Trace and minor elements in sphalerite

Sulitjelma:(NC5835, NC6005, Sulis 1b, Sulis 2a, Sulis 2b)

No banding or preferential grain orientations were observed, but inter-granular and intra-granular fracturing was observed throughout the samples, fractures were seen running through pyrite, sphalerite and pyrrhotite mineral grains (see Figure 4 A, C, D, E and F).

The mineral grains found in the samples from Sulitjelma are coarser grained than the grains in Røros, and contain a few pyrite grains that are extremely coarse-grained and very angular (see Figure 4 A and B). In these samples the large pyrite grains can be found as both strongly angular polyhedral shapes and as rounded circular shapes (see Figure 4 A, B, E and F), indicating that the pyrite grains may have recrystallised into larger grains during the metamorphism but subsequently underwent ductile deformation. Notably the pyrite grains appear to be more angular and polyhedral shaped in places where pyrite dominates (Figure 4 A and B) but appear to be more rounded where the pyrite grains are surrounded by other minerals, mostly chalcopyrite and sphalerite. This suggests that the enclosing minerals influenced the extent to which brittle verses ductile deformation acted on the pyrite grains, with the softer sphalerite and chalcopyrite allowing for more ductile deformation. Along with pyrite, chalcopyrite and sphalerite make up the majority of the sulphides in the samples, unlike the pyrites however, the chalcopyrite and sphalerite are far more amorphous in shape, filling in the gaps between pyrite grains (Figure 4 E and F). Of particular note was that easily observable 'chalcopyrite disease' could be seen in almost every sphalerite grain (Figure 4 C and D) in the samples, more so than in any other deposit analysed.

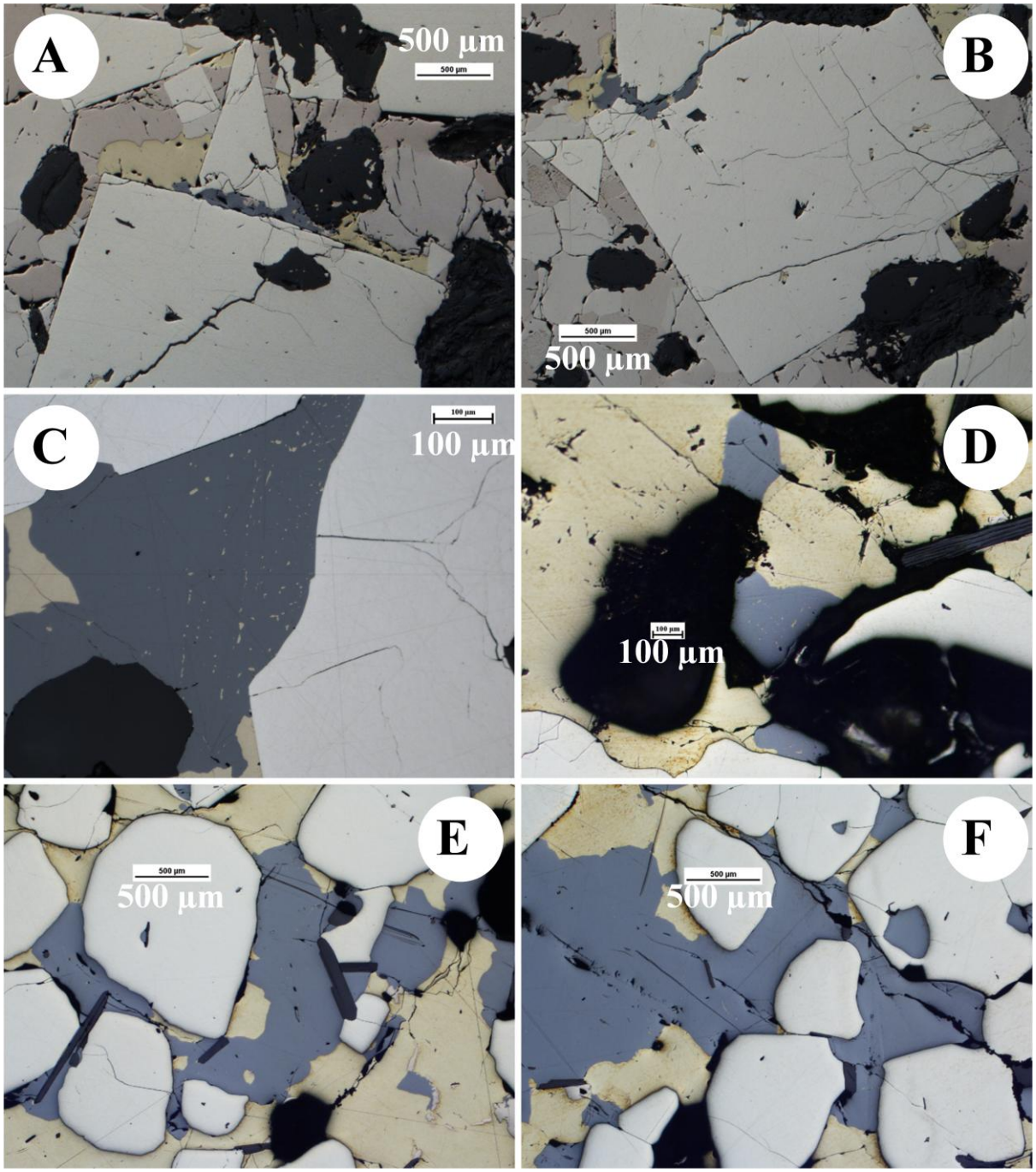

Figure 4: Photomicrographs in reflected light of the samples from Sulitjelma. (A) and (B) show the large, angular polyhedral shaped pyrite grains which can be found in some parts of the samples. (C) shows an example of the chalcopyrite disease which is found in many of the larger sphalerite grains. (D-F) show the general nature of the samples, with most of the large pyrite grains occurring as amorphous to semi-amorphous grains, whereas the chalcopyrite and sphalerite fill the matrix between the pyrite. (F) also shows an example of sphalerite inclusions in pyrite, which occur in many places in the samples.

Trace and minor elements in sphalerite

Mofjellet:(Mo2, Mo5, Mo10)

No banding or preferential grain orientations was observed, but extensive intergranular and intraganular fracturing was observed throughout the samples, fractures were seen running through grains of pyrite, sphalerite and pyrrhotite (see Figure 5 A, C, D, E and F), these samples were significantly more fractured than the Sulitjelma samples.

The mineral grains found in the samples from Mofjellet are mostly of similar size to the grains found in Røros except for the presence of some quite large sphalerite and pyrite grains in some places. Unlike the mineral grains found in Mt Isa and Røros quite a few of the mineral grains found in these samples have a straight edge or two (see Figure 5 D and F). The amorphous to semi amorphous nature of the mineral grains in these samples indicate it is likely overprinting has occurred, and the extensive fracturing indicates that significant deformation of the deposit had occurred at some point after the formation of the deposit.

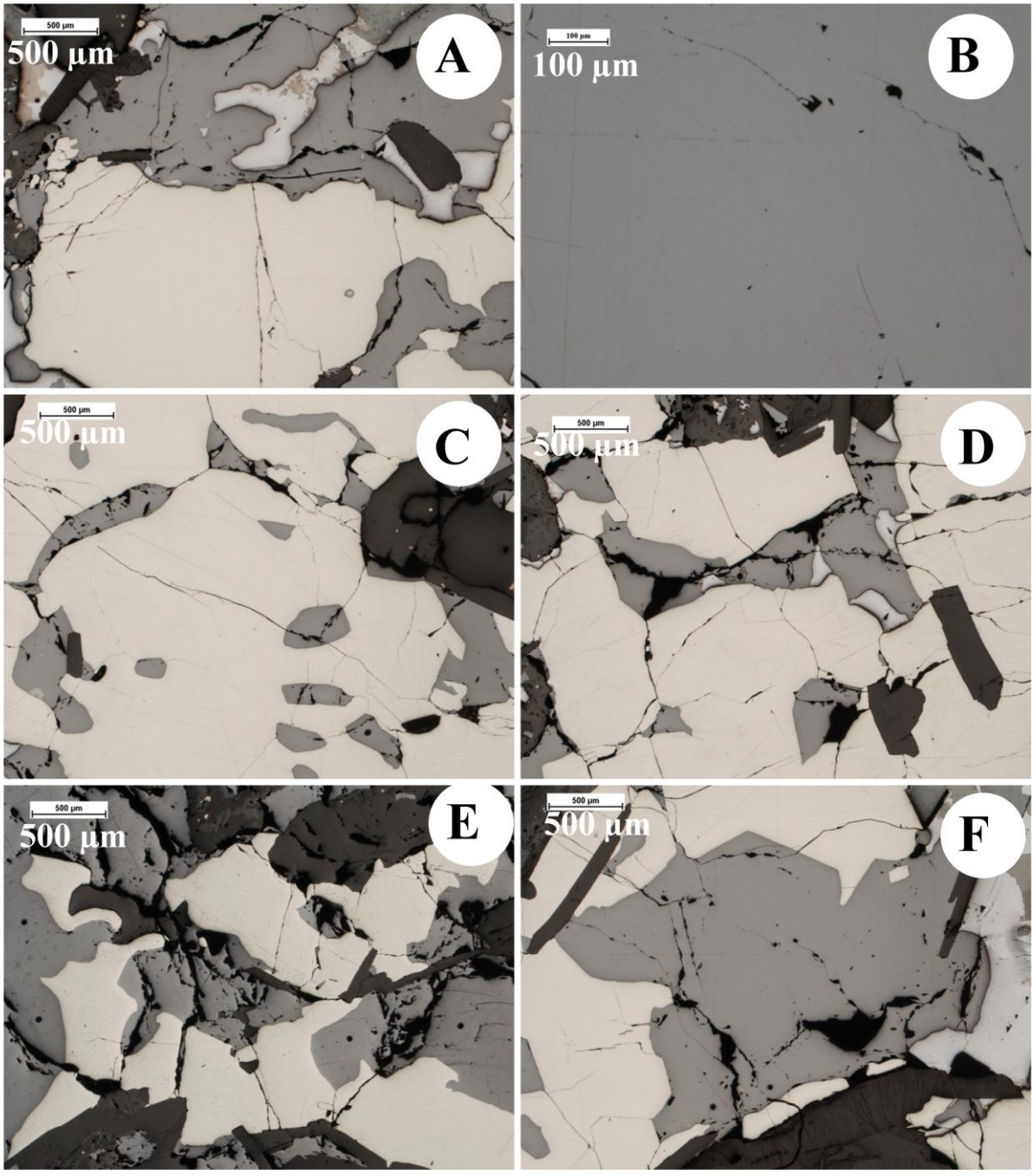

Figure 5: Photomicrographs in reflected light of the samples from Mofjellet. (A) shows the general nature of the samples, with large grains that are partially amorphous, but do show some straight edges in places. (B) shows a close up of the centre of a large sphalerite grain, showing an absence of 'chalcopyrite disease'. (C-F) show the general nature of the sphalerite in the samples, note that the sphalerite and pyrite grains occur both as amorphous and semi amorphous grains. (D) and (F) also show fractures running though sphalerite and into pyrite grains and vice versa.

Bleikvassli:(Bv1, V59.197, V60.446 and V61.538)

The mineral grains in the samples from Bleikvassli were consistently coarse grained, apart from some fine grained inclusions in larger grains. No overall structural features

were observed, some fractures were found within some of the larger pyrite grains, but these fractures mostly seem to terminate at the grain boundaries of the pyrite grains. Extensive signs of quartz overprinting of the sphalerite and pyrite were observed, as shown in Figure 6 A, B and D. The pyrite mineral grains occurred as angular polyhedral shapes where they had not been over printed, all other minerals showed either rounded or amorphous shapes. The extensive overprinting of the sulphides by gangue minerals (mostly quartz) together with the large grainsize of the pyrite where not overprinted and the tetrahedrite within galena sporadically found in places (Figure 6 E) indicates possible strong prograde recrystallisation followed by retrograde overprinting.

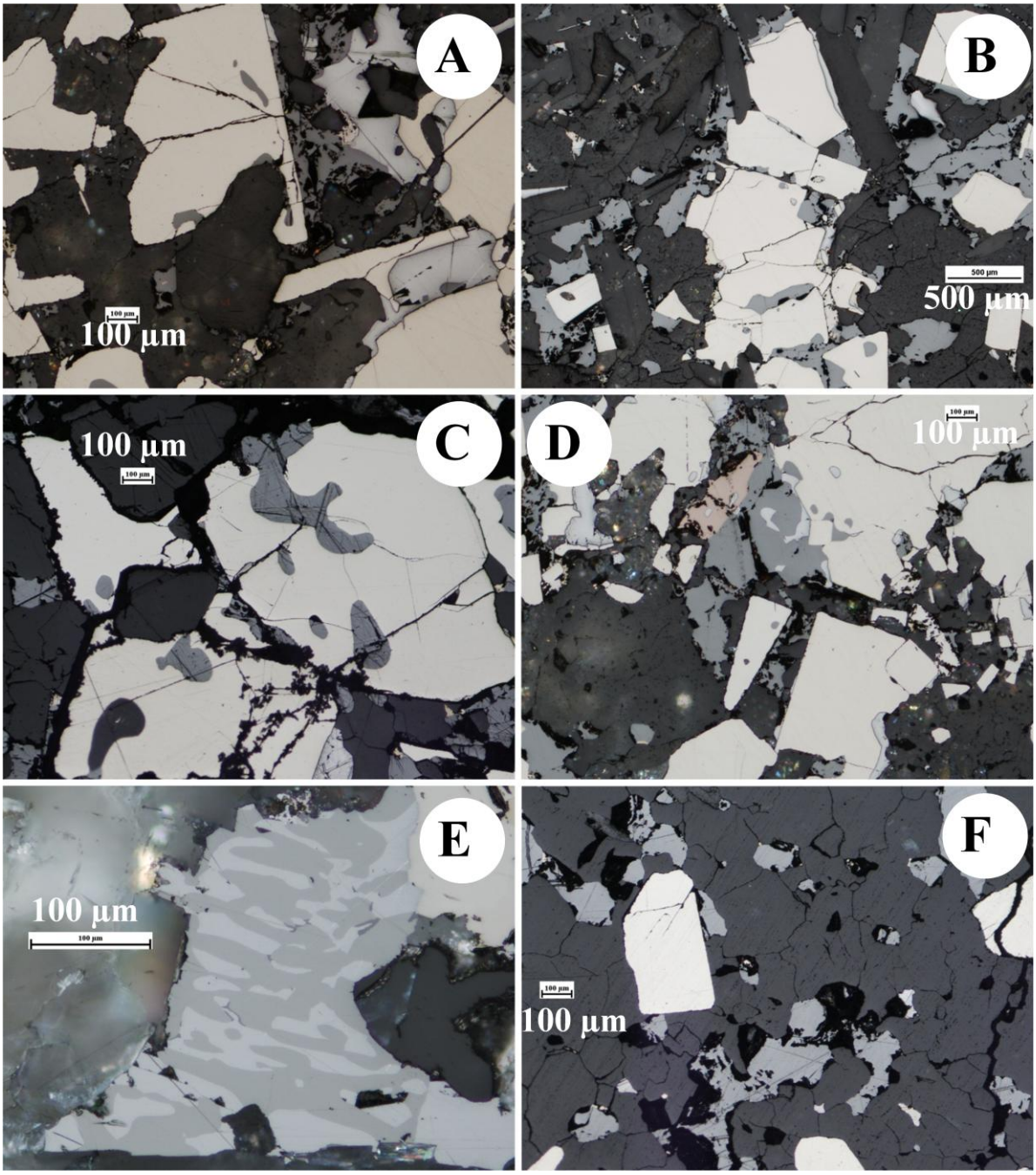

Figure 6: Photomicrographs in reflected light of the samples from Bleikvassli. (A) and (B) show the general overview of the samples, particularly the overprinting of the sulphides by non-sulphide gangue material that pervades the samples. (C), (D) and (F) show how sphalerite in particular relates to the other minerals, with it mostly occurring alongside and/or inside other sulphide minerals such as pyrite and pyrrhotite, although it is occasionally found surrounded by non sulphides such as in (F). (E) shows an exsolution pattern of tetrahedrite and galena a that was found in a few places.

Broken Hill:(BH218 and BH221)

The mineral grains in the samples from Broken Hiil are extremely coarse-grained, such that some large grains could not be pictured in their entirety even using the lowest

magnification of the optical microscope. While the pyrite grains were fracture free, extensive triangular cleavage pits and distinctive cleavage lines of were found to occur in the galena, which dominates large regions of the samples, few fractures are found in the other minerals in the samples. Extensive signs of galena replacing sphalerite were observed (Figure 7 C and F), the extent of the replacement varies in different regions of the samples. The mineral grains occur as amorphous blobs throughout both samples, what mineral shapes may have existed appear to have been extensively altered during one or more overprinting stages.

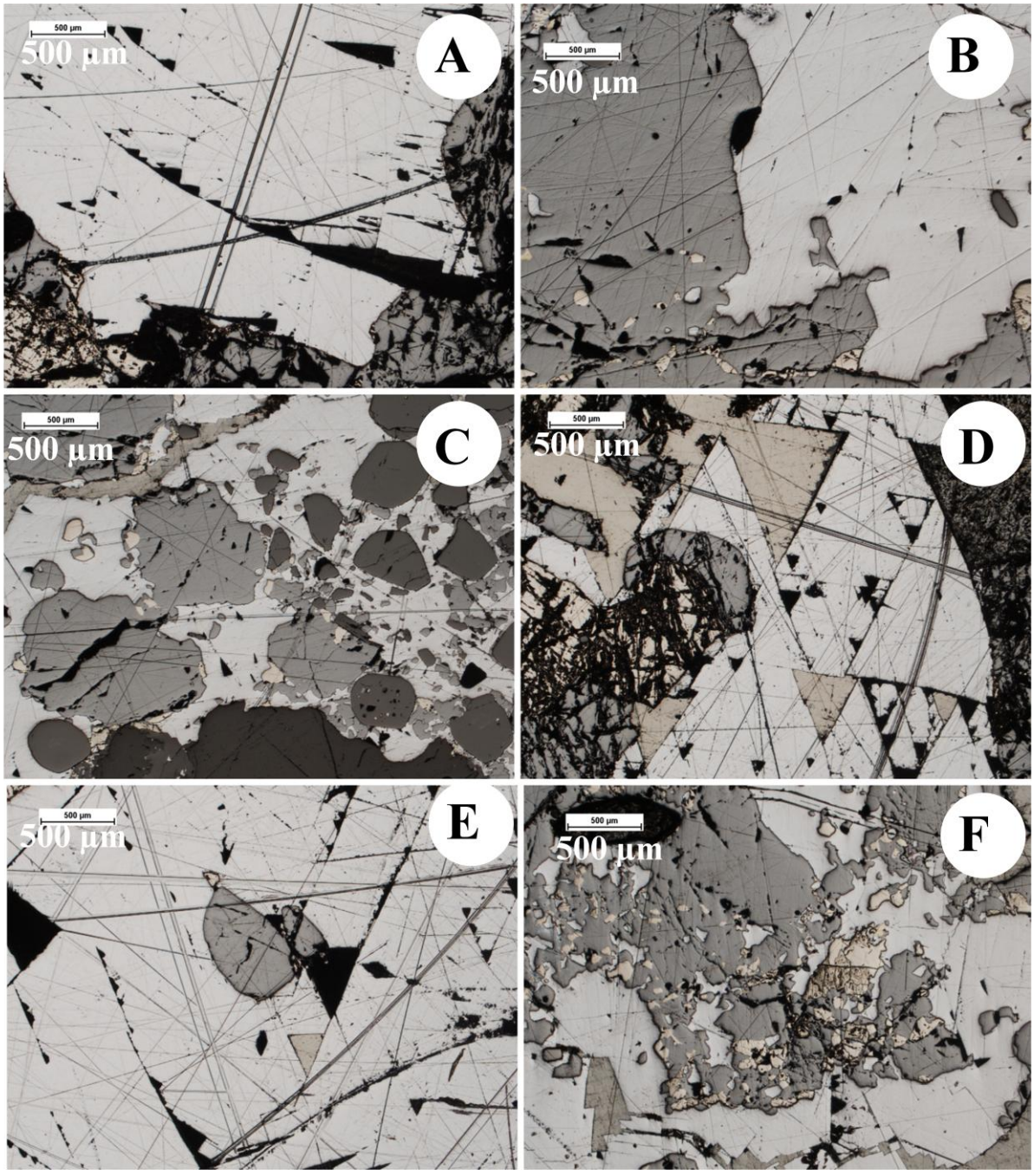

Figure 7: Photomicrographs in reflected light of the samples from Broken Hill. (A) shows just one part of the extremely-coarse galena which can be found in these samples. (B) shows the contact between a very large galena grain and a very large sphalerite grain, the sphalerite grains in these samples can get as large as the galena grains. (C) shows grains of sphalerite within a matrix of galena, note the irregular margins which suggest replacement of sphalerite by galena. (D) and (E) show the triangular cleavage patterns which run through the galena in the samples. However (E) shows that the sphalerite inclusions in the galena are unaffected by the cleavage. (F) shows sphalerite being replaced by galena.

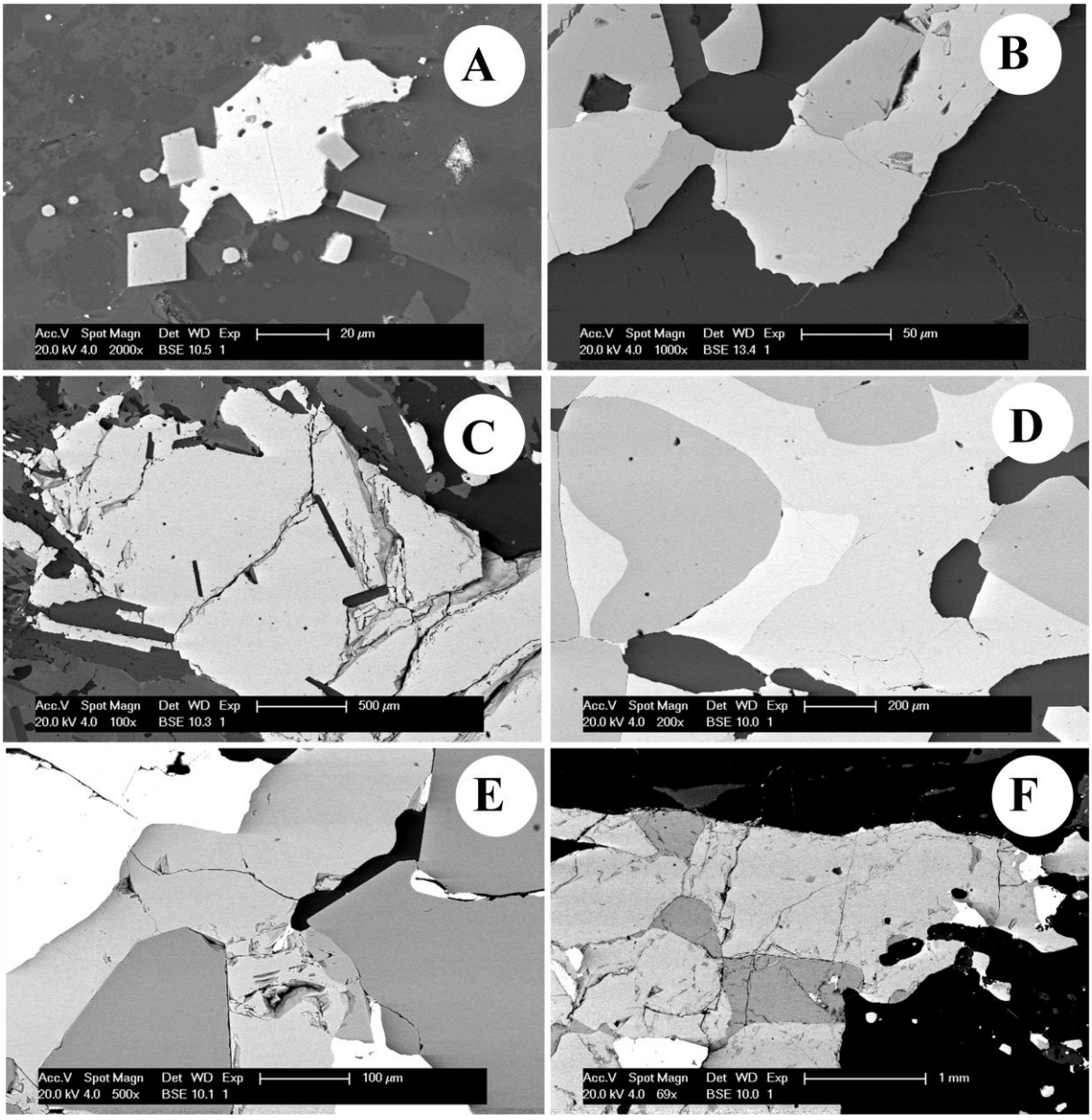

Figure 8: Back-scatter electron (BSE) images of sphalerite from the 6 deposits. (A) is a picture of a sample from Mt Isa. (B) is a picture of a sample from Røros. (C) is a picture of a sample from Mofjellet. (D) is a picture of a sample from Sulitjelma. (E) is a picture of a sample from Bleikvassli. (F) is a picture of a sample from Broken Hill. In all pictures the lightest grey (not white) is sphalerite.

Elemental distribution results:

During the course of this study, the LA-ICP-MS instrument was used to analyse for the elemental concentrations of the minor and trace elements of interest. A large amount of information was collected on these elemental concentrations and as such the full lists of

data are shown in Appendix A. A summary of the mean concentrations and the standard deviations of the data for each element of interest for each sample are shown in Table 2.

MEAN CONCENTRATIONS (ppm)

Deposit	Sample	Mn	Fe	Co	Cu	Ga	Se	Ag	Cd	In	Sn	Sb	Hg	Tl	Pb	Bi
Mt. Isa	5984A (n=20)	55	45779	bdl	121	bdl	bdl	23	1879	8.9	bdl	26	113	1.31	12041	0.35
	5984B (n=20)	297	47790	bdl	63	0.449	bdl	66	1967	25	bdl	87	65	3.44	56005	1.4
Roros	STO17504 (n=18)	469	74576	226	12619	1.34	91	11	1310	40	2.95	0.26	39	0.10	440	69
	STO17505 (n=20)	492	57768	32	457	1.34	121	4.1	1187	28	0.637	0.83	41	bdl	29	3.2
	STO17506 (n=20)	1135	64579	127	40	5.59	47	1.7	1139	8.3	0.838	0.43	25	bdl	2.9	2.0
Sulitjelma	NC5835 (n=20)	776	74406	27	13451	10.5	bdl	6.4	1473	18	4.88	3.5	104	bdl	3.2	0.18
	NC6005 (n=10)	727	60213	99	605	2.06	100	5.9	1786	90	1.76	2.3	38	bdl	4.4	0.78
	Sulis 1b (n=20)	911	81311	31	574	7.29	bdl	4.3	1524	17	bdl	1.4	44.4	bdl	1.0	0.08
	Sulis 2a (n=16)	1275	56465	27	329	1.31	71	4.3	3113	5.1	bdl	1.3	235	bdl	1.3	0.52
	Sulis 2b (n=20)	1351	72921	31	67	1.47	37	3.4	2873	5.3	bdl	0.96	178	bdl	3.3	1.2
Mofjell	Mo2 (n=18)	589	32142	bdl	9.1	1.21	bdl	0.99	2012	1.7	bdl	bdl	173	bdl	22	bdl
	Mo5 (n=20)	1446	59851	bdl	8.0	1.84	bdl	1.4	2110	2.3	bdl	bdl	212	bdl	1.2	bdl
	Mo10 (n=20)	957	43640	bdl	6.5	1.32	bdl	0.99	1988	1.2	bdl	bdl	290	bdl	2.1	bdl
Bleikvassli	Bv1 (n=20)	313	62698	bdl	76	18.6	bdl	2.6	1405	56	5.04	1.3	135	bdl	22	bdl
	V59.197 (n=20)	758	72318	bdl	115	5.94	bdl	2.1	1273	119	bdl	0.75	155	0.013	2.6	0.01
	V60.446 (n=20)	2791	54962	bdl	75	1.95	bdl	5.3	1458	87	2.50	3.8	108	bdl	2876	bdl
	V61.538 (n=20)	2079	63272	bdl	47	5.83	bdl	1.4	1560	52	4.96	0.60	68	bdl	0.36	bdl
Broken Hill	BH218 (n=20)	1705	74090	62	34	6.69	bdl	1.9	1667	2.9	bdl	0.11	21	bdl	1.9	bdl
	BH221 (n=20)	775	59203	93	28	4.7	bdl	4.0	2824	2.6	bdl	0.26	41	bdl	2.7	bdl

STANDARD DEVIATIONS ON THE MEANS

Deposit	Sample	Mn	Fe	Co	Cu	Ga	Se	Ag	Cd	In	Sn	Sb	Hg	Tl	Pb	Bi
Mt. Isa	5984A	14.8	2499	bdl	196	bdl	bdl	25	128	4.5	bdl	35	29	2.08	43681	1.26
	5984B	585	28192	bdl	102	0.30	bdl	172	204	8.6	bdl	229	32	8.75	169040	4.34
Roros	STO17504	584	35700	24.1	40508	1.6	25.2	11	71	11	4.07	0.29	9.8	0.14	676	143
	STO17505	68	2661	1.96	1418	0.4	30.9	2.9	37	2.3	0.623	1.0	3.7	bdl	61	2.89
	STO17506	30	1048	9.9	39	1.1	6.6	1.8	15	0.16	0.244	0.7	3.3	bdl	5.2	3.24
Sulitjelma	NC5835	70.5	42445	7.51	45565	9.0	bdl	12	285	5.3	14.7	5.0	53	bdl	6.7	0.26
	NC6005	263	7179	35.2	493	2.1	24.7	9.0	121	21	0.876	2.6	6.4	bdl	3.7	0.55
	Sulis 1b	147	8708	10.8	1518	4.7	bdl	8.8	131	2.2	bdl	1.4	5.0	bdl	1.6	0.09
	Sulis 2a	201	5297	4.2	1261	0.29	32.7	4.6	293	1.7	bdl	1.6	48	bdl	1.8	0.98
	Sulis 2b	190	10483	7.0	151	0.70	14.6	2.4	257	1.4	bdl	1.0	25	bdl	5.4	4.55
Mofjell	Mo2	216	3671	bdl	6.9	2.0	bdl	0.52	141	0.07	bdl	bdl	99	bdl	71	bdl
	Mo5	314	2709	bdl	3.0	0.42	bdl	1.1	150	0.17	bdl	bdl	60	bdl	0.88	bdl
	Mo10	46	3818	bdl	2.0	0.39	bdl	0.12	92	0.06	bdl	bdl	88	bdl	4.6	bdl
Bleikvassli	Bv1	104	3250	bdl	29	1.37	bdl	2.7	75	2.5	9.40	2.5	26	bdl	61	bdl
	V59.197	78.1	5187	bdl	7.2	0.88	bdl	1.1	27	6.7	bdl	1.0	29	0.027	6.6	0.01
	V60.446	197	4259	bdl	17	0.39	bdl	13	74	18	3.34	7.1	21	bdl	12847	bdl
	V61.538	245	4376	bdl	4.9	0.34	bdl	0.58	48	1.6	3.98	1.3	5.2	bdl	0.59	bdl
Broken Hill	BH218	94.8	2016	7.78	7.6	0.27	bdl	1.6	45	0.08	bdl	0.09	5.8	bdl	2.5	bdl
	BH221	67	8980	9.26	7.5	0.47	bdl	2.9	142	0.17	bdl	0.31	21	bdl	3.8	bdl

Table 2: Summary of LA-ICP-MS minor and trace element data for each sample (means and standard deviations for each element), bdl is listed where majority of ablation spots gave results below minimum detection limits.

Figure 9 shows a graphical representation of the mean data shown in Table 2, for ease of comparison. Standard deviation could not be shown due to the standard deviation exceeding the mean in some cases and negative numbers cannot be graphed logarithmically.

Trace and minor elements in sphalerite

5984A

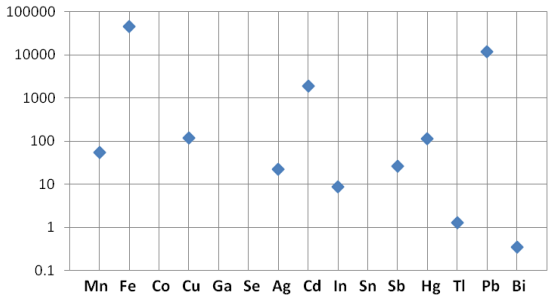

5984B

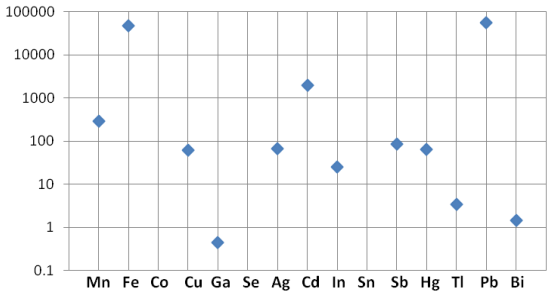

STO-175-04

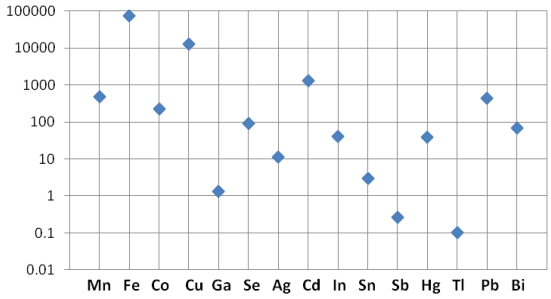

STO-175-05

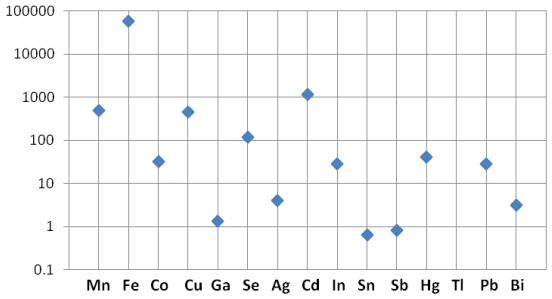

STO-175-06

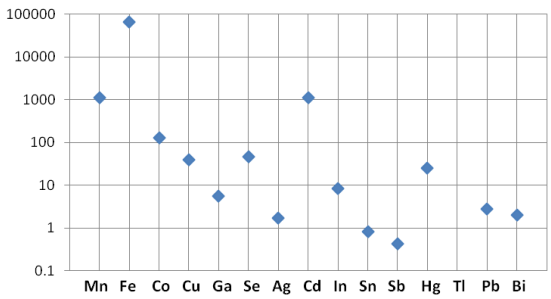

NC5835

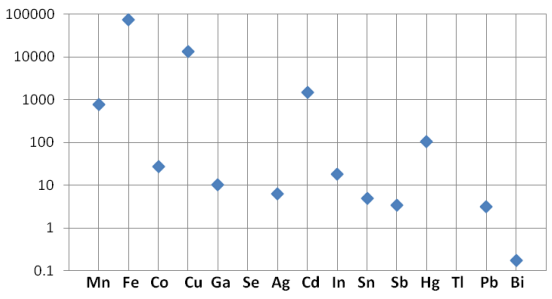

NC6005

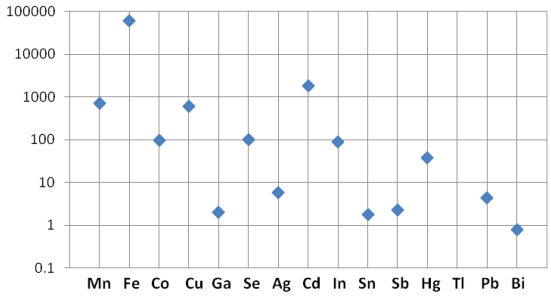

Sulis 1b

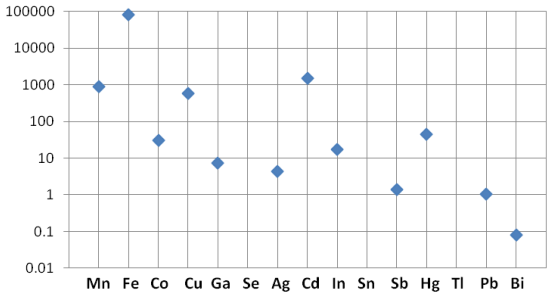

Sulis 2a

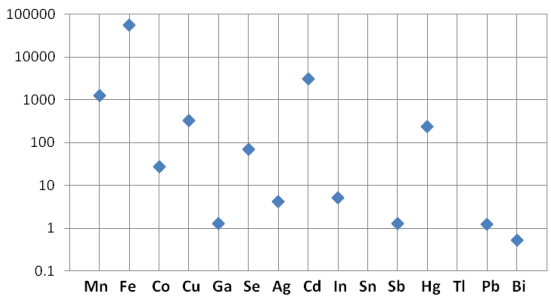

Sulis 2b

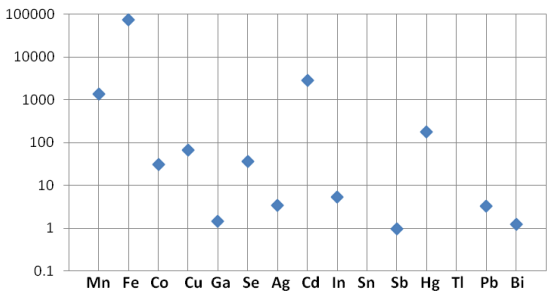

Trace and minor elements in sphalerite

Mo2

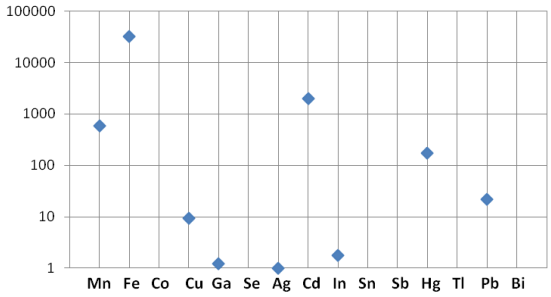

Mo5

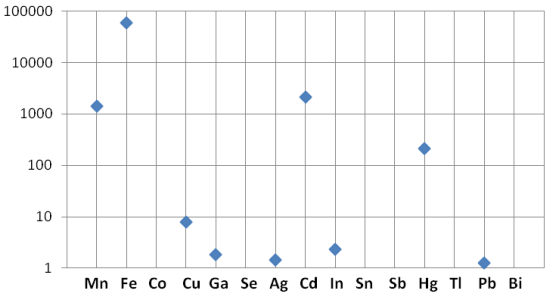

Mo 10

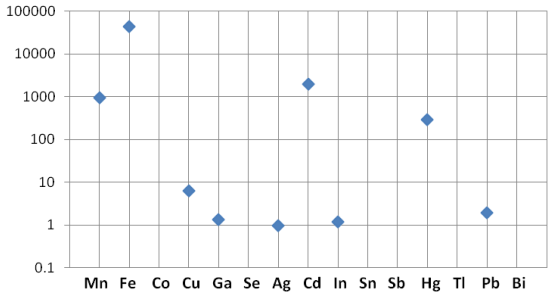

Bv1

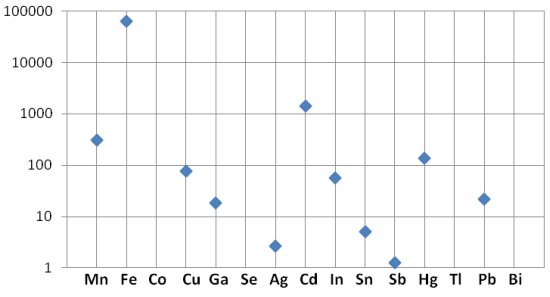

V59.197

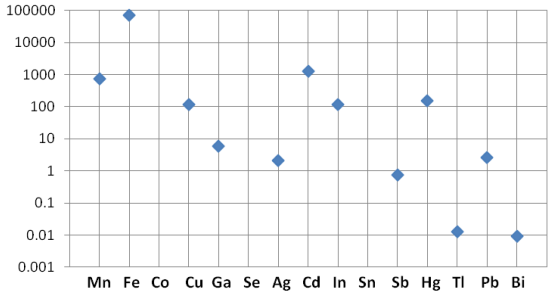

V60.446

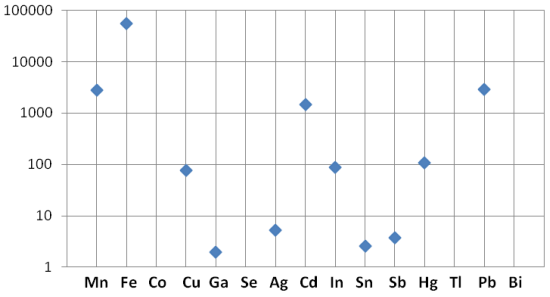

V61.538

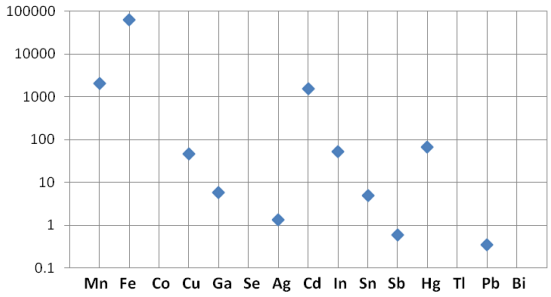

BH218

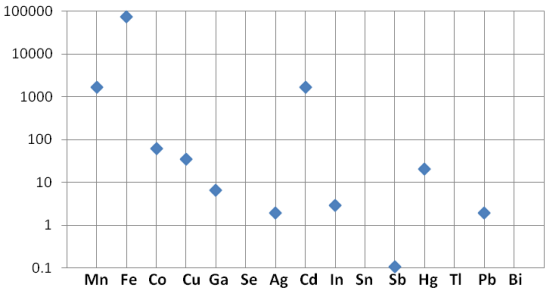

BH221

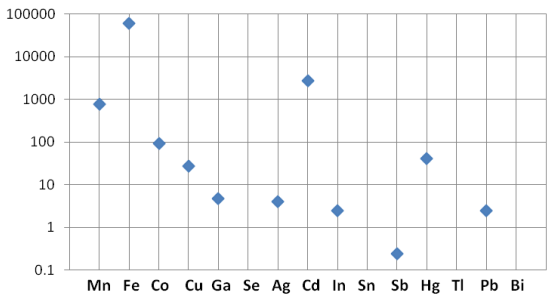

Figure 9: Graphical representations of the mean abundance of Mn, Fe, Co, Cu, Ga, Ag, Cd, In, Sn, Sb, Hg, Tl, Pb and Bi within each sample in ppm on a logarithmic scale. Where the elemental abundances were mostly below detection limits no mark is displayed. The rock samples 5984A, 5984B are from the Mt Isa ore deposit, STO-175-04, STO-175-05 and STO-175-06 are from the Røros ore deposit, NC5835, NC6005, Sulis 1b, Sulis 2a and Sulis 2b are from the Sulitjelma ore deposit, Mo2, Mo5 and Mo10 are from the Mofjellet ore deposit, Bv1, V59.197, V60.446 and V61.538 are from the Bleikvassli ore deposit, and BH218 and BH221 are from the Broken Hill ore deposit.

As one of the main goals of this study is to attempt to identify any elemental relationships, elemental comparisons were made for all of the main minor elements. Figure 10 and Figure 11 show some of these comparisons, most of which resulted in no clear relationships being identified.

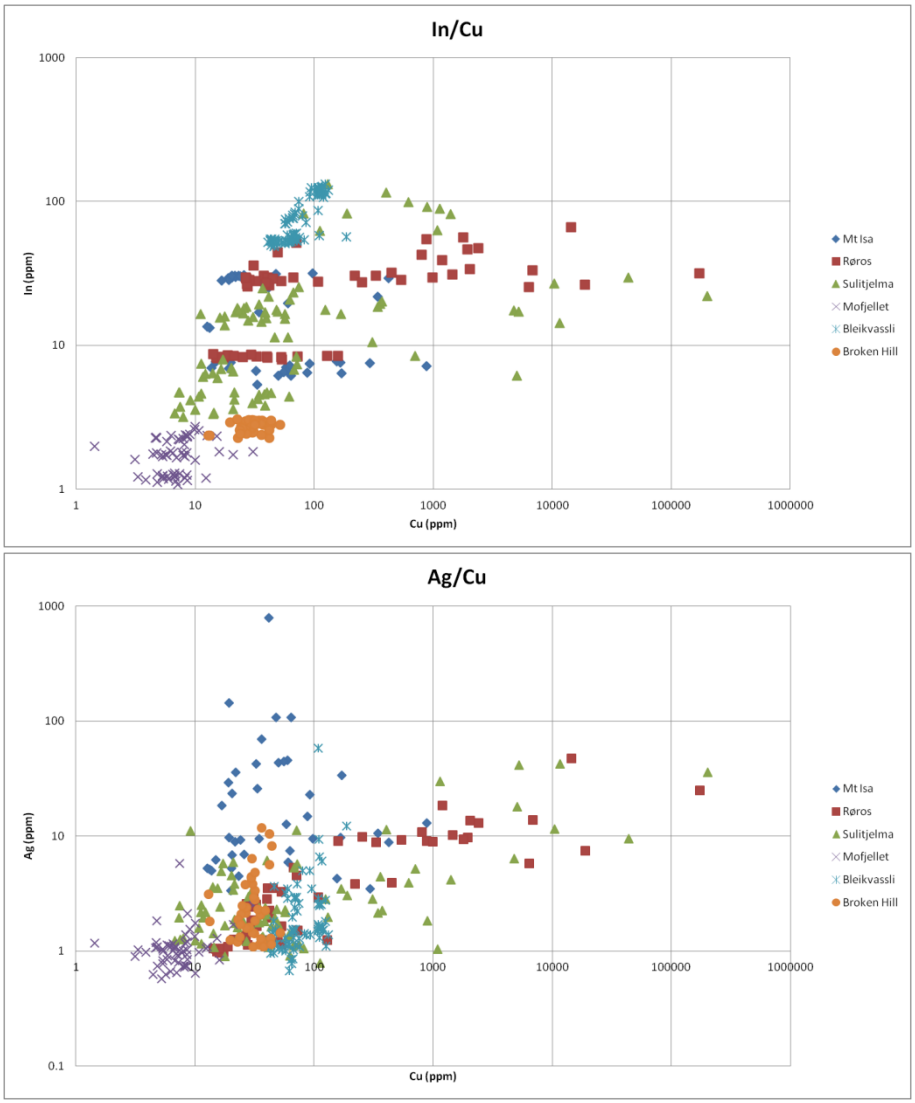

Trace and minor elements in sphalerite

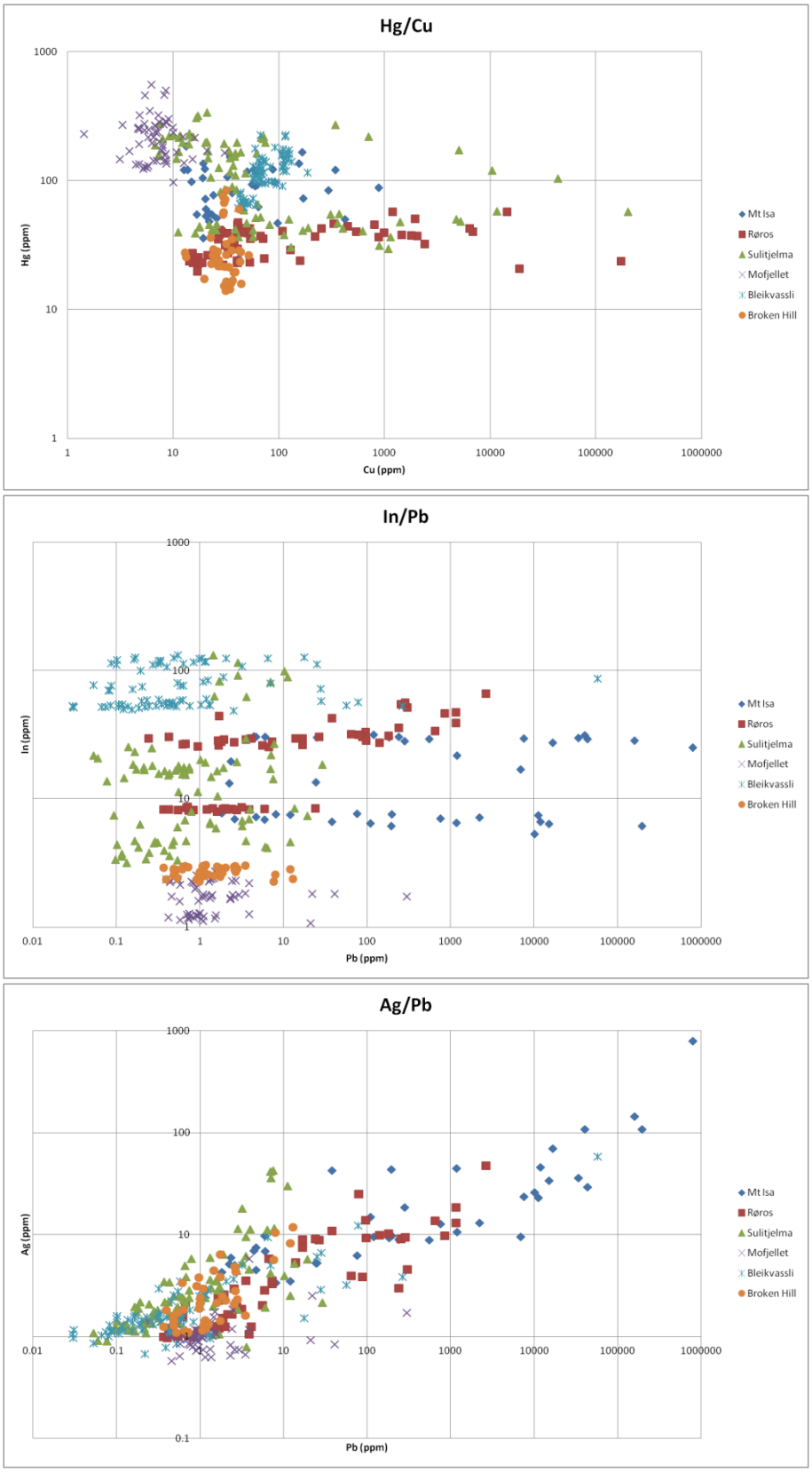

Trace and minor elements in sphalerite

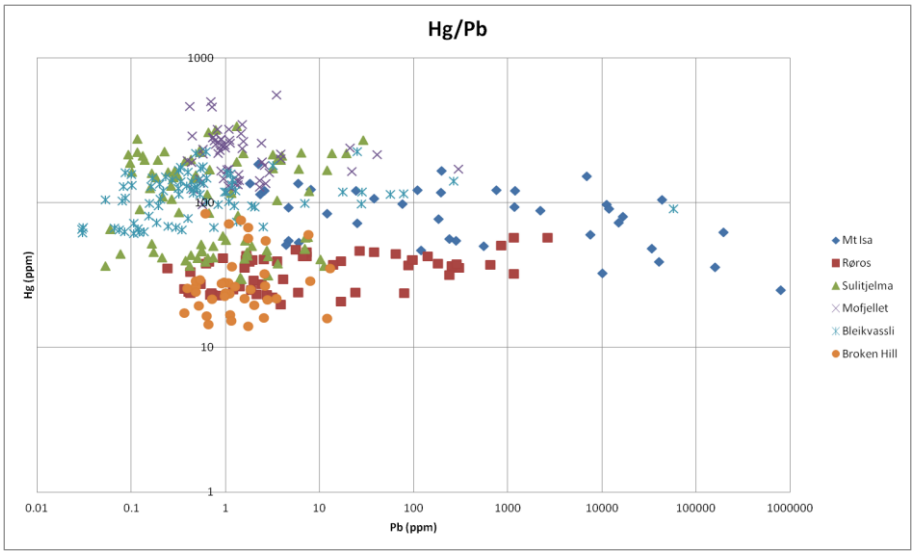

Figure 10: Graphical comparisons of the abundance in ppm of some elements of interest compared to Cu and Pb, which are considered to exist mostly in inclusions in sphalerite. Data points from all samples shown. The two axes display the abundance of different elements logarithmically so that they can be compared easily. Note that a moderately strong positive correlation between In and Cu and between Ag and Cu, and a quite strong positive correlation between Ag and Pb is observable.

The relationships between In and Cu, Ag and Cu, and Ag and Pb shown in Figure 10 indicate that these elements are most likely at least partially linked via some process.

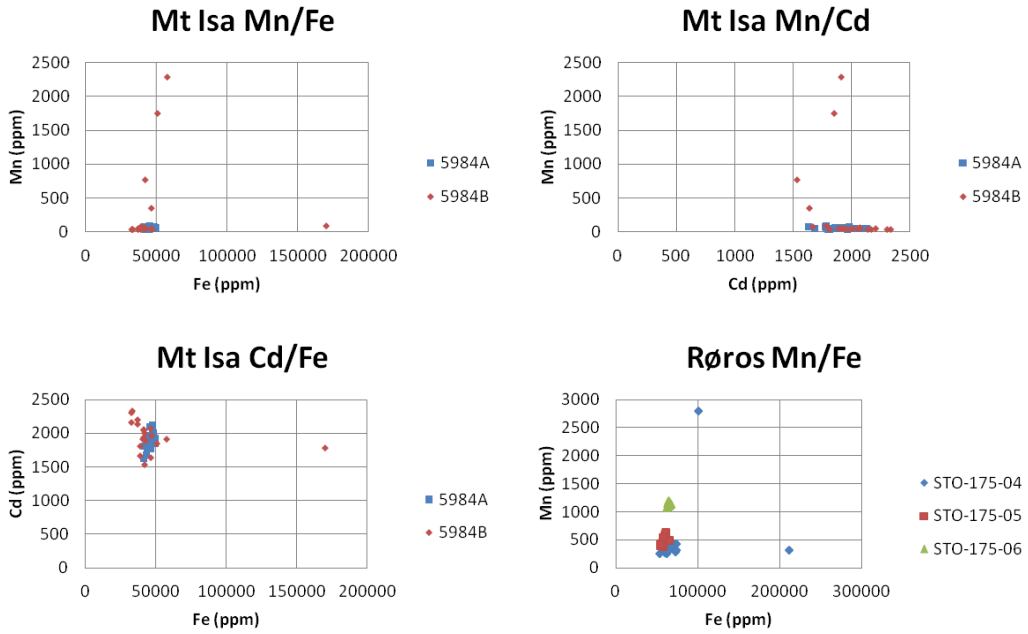

Trace and minor elements in sphalerite

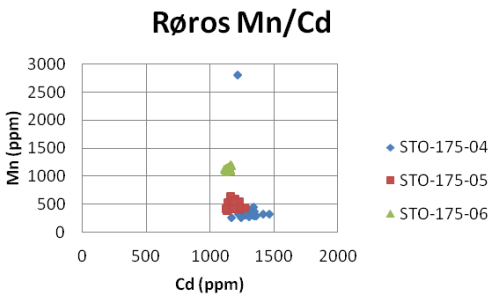

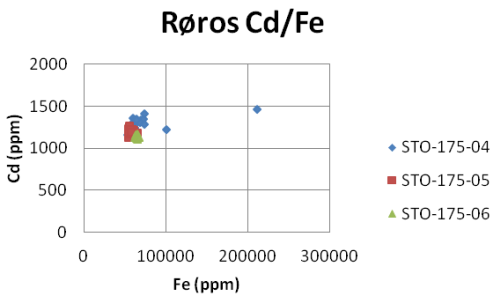

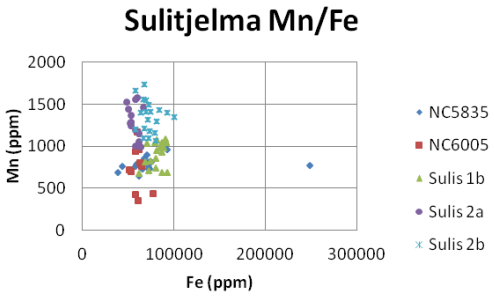

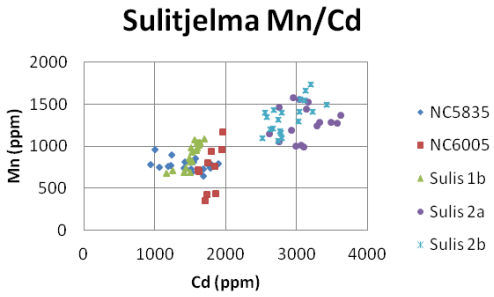

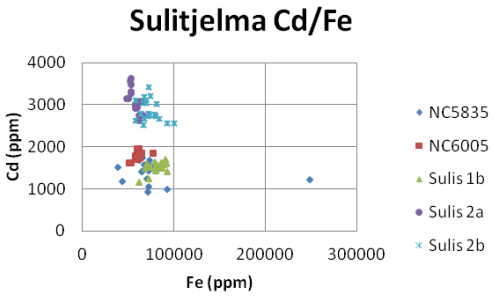

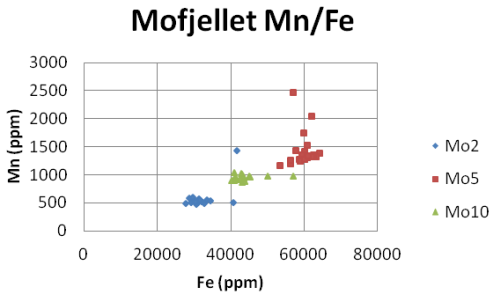

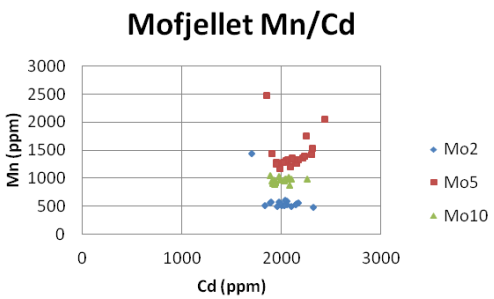

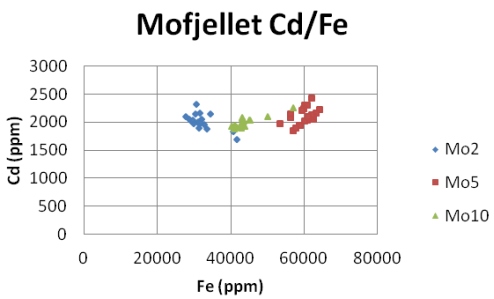

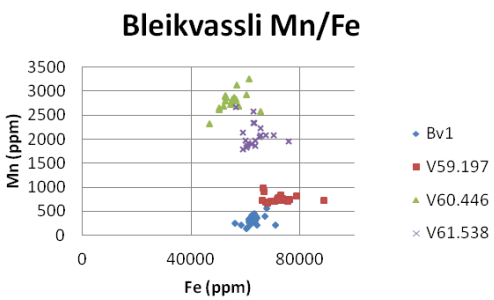

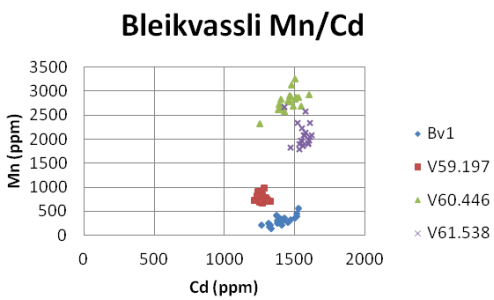

Trace and minor elements in sphalerite

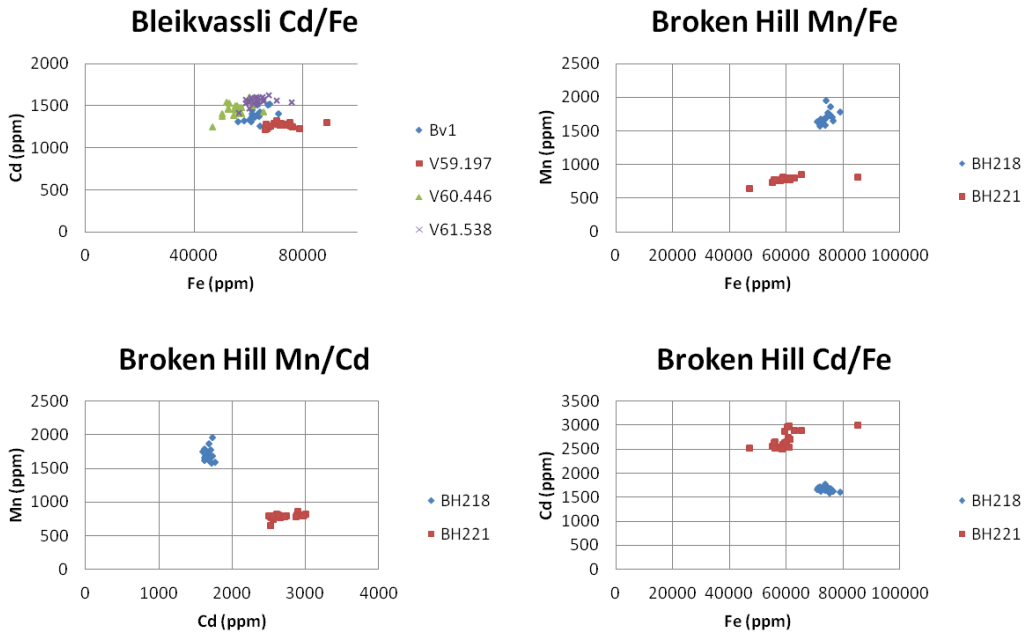

Figure 11: Binary element plots demonstrating how common minor elements in sphalerite compare to each other in each of the deposits types. Note that there does not appear to be any consistent trends present which link these elements. The data from some samples from the same deposit cluster together, such as those from Røros, while data from Sulitjelma is more spread out.

DISSCUSSION:

Minor and trace element abundances:

As Figure 9 shows, the average concentrations of the three most abundant minor elements found in sphalerite (Mn, Fe, Cd) are relatively constant between samples from different deposits. The sample means all lie within the same order of magnitude for the three elements. Table 2 shows that the sample means for Mn vary more than Fe or Cd between individual samples, even though Mn concentrations are relatively constant within sample as shown by the generally low standard deviations.

Trace and minor elements in sphalerite

Iron is the most common minor element in sphalerite and occurs as wt.% in most sphalerite, including the sphalerite analysed in this study. There exists a partial solid solution between Fes and ZnS, with reports of up to 56 mol.% FeS replacing ZnS under laboratory conditions (Vaughan & Craig 1978). Manganese and cadmium substitutions extend to around 15 and 14 mol.% respectively (Tauson *et al.* 1977; Patrick *et al.* 1998).

Manganese is a relatively common component of sphalerite, yet published data sets show that there is a broad variation in concentrations in different sphalerite samples, ranging from trace amounts to several wt.%, with MnS concentrations in some epithermal deposits exceeding 5% (Cook *et al.* 2009). Mn incorporation into sphalerite occurs via cation exchange ($Zn^{2+} \leftrightarrow Mn^{2+}$), although as alabandite (MnS) is not isostructural with sphalerite there is an upper limit to incorporation at about 7mol% (Sombuthawee *et al.*1978). The present study has shown Mn abundances ranging from less than 30ppm to more than 3000ppm. The unusually high standard deviations compared to means for samples Mo2, STO17504 and 5984B all occur as a result of a small number of outlier data points which have much higher values than the other data points taken from those samples (See Appendix A). The removal of four anomalous data points from 5984B would, for example, give a similar mean and standard deviation as 5984A.

The consistent cadmium concentrations found in every sample, as shown by the similar means and relatively low standard deviations (Table 2) are consistent with published work showing that in stratiform ores Cd tends to on average range from 0.1 to 5 wt.%, although in MVT deposits and in sphalerite rich veins in carbonate rocks cadmium can

occur at much higher abundances and can be important sources for cadmium produced as a by product (Schwartz 2000; Ye *et al.* 2012).

The cobalt ion is similar in size to that of Fe (Cook *et al.* 2009) and as such can be expected to be substituted within sphalerite in moderate amounts in all samples. However, as Figure 9 an Table 2 show, while cobalt was found to occur in the tens to hundreds of ppm in ores from Røros, Sulitjelma and Broken Hill, it was mostly below detection limits in samples from Mt Isa, Mofjellet and Bleikvassli, possibly indicating that cobalt incorporation is restricted by its availability in the source rock and as such would be higher in Co-rich mafic volcanic rocks (VMS type) than it would be in comparatively Co-poor sedimentary sequences (SEDEX type).

Copper is not widely considered to readily incorporate itself into the sphalerite lattice in any great abundance and is more often found within sphalerite grains as tiny inclusions of chalcopyrite, dubbed 'chalcopyrite disease' (Barton & Bethke 1987) (See Figure 4 C & D for examples of chalcopyrite disease). This implies it is possible that the variations in copper abundance are mostly due to variations in the density of chalcopyrite contamination rather than due to real lattice-bound copper in sphalerite, especially where large variations in Cu concentrations are observed. Copper concentrations are highly variable between ablation spots in samples from the Mt Isa, Røros and Sulitjelma deposits, individual spot analyses for STO-175-04 , STO-175-05, Sulis 1b, Sulis 2b and NC5835 show highly variable copper values, ranging from <30 ppm to >700 ppm. STO-175-05 and Sulis 1b have values exceeding 5000 ppm copper while STO-175-04 and NC5835 even have ablation spots exceeding 10,000 ppm (or ~1wt.%). The highest

single value is >40,000 ppm Cu. These anomalously high copper readings skew the average concentrations drastically. This would be expected if heterogeneously distributed 'chalcopyrite disease' was strongly affecting the measured concentrations in these samples.

In Bleikvassli, Mofjellet and Broken Hill average copper concentrations are lower and much less variable between ablation spots The greater homogeneity of copper concentration in samples from these three deposits is consistent with the lack of observed 'chalcopyrite disease' and so this copper can be attributed to substitution within the sphalerite lattice.

Gallium can occur at up to 20 mol% in solid solution as Ga_2S_3 in sphalerite (Kramer *et al.* 1987), it has been reported to occur in higher concentrations in carbonate hosted and some MVT sphalerite deposits, neither of which are represented in the 6 deposits samples (Cook *et al.* 2009). The abundance of gallium appears to be relatively constant between samples, coming in with an average between 1 and 19 ppm for all samples. No apparent elemental relationships with other elements were found in the results.

Like Ga, the abundance of silver is also relatively constant, occurring with an average of between 1 and 11 ppm in all samples except those from Mt. Isa. The Mt Isa samples show strong Ag enrichment of the sphalerite, indicating that the sphalerite is likely an important Ag carrier in this ore. This contrasts with the Broken Hill samples where sphalerite is Ag poor.

Trace and minor elements in sphalerite

Variation in the indium concentration between different samples is greater than that of Ga or Ag, but the element shows homogeneity between ablation spots from the same sample as shown by the low standard deviations in Table 2. Indium is generally considered to be incorporated within sphalerite via the coupled substitution $2Zn^{2+} \leftrightarrow Cu^{+} + In^{3+}$ (Sombuthawee *et al.* 1987).

Selenium was found to occur at mostly above detection limits in only Røros and some Sulitjelma samples. However, due to very high minimum detection limits (40-80ppm in most cases, over 190ppm for some ablation spots) for Se, it is difficult to draw conclusions from the results.

Mercury was found to be significantly above detection limits in all samples. The relatively consistent (less than 300 ppm difference between the lowest and highest mean values for all samples) results suggest that mercury not drastically affected by the abundances of other elements and the mostly low standard deviations relative to the means indicates that the mercury is most likely lattice-bound.

Thallium was found to be below detection limits or close to detection limits in all samples except those from Mt Isa. As shown by the standard deviations for these two deposits being significantly higher than the means, in the Mt Isa deposits thallium abundance varied significantly between ablation spots, this heterogeneity suggests that much of the thallium in the Mt Isa deposits may have been inclusion related (for instance, one of the ablation spots for 5984B was >39 ppm while ten of the spots were <1 ppm).

Trace and minor elements in sphalerite

Lead concentrations vary significantly between different samples from the same deposit and even between different ablation spots in the same sample. These highly heterogeneous results, coupled with noisy time resolved LA-ICP-MS depth spectra, indicate that lead dominantly occurs as micro- to nanoscale inclusions of galena and/or other Pb-bearing sulphides that can significantly skew the data depending on their density. Of particular concern is that some extremely high Pb concentrations were measured in some individual ablation spots. Examples include STO-175-04, in which 8 out of 18 ablation spots gave Pb concentrations of exceeding 250 ppm and 3 were >1,000 ppm, and sample V60.446 in which one particular spot gave 57,458 ppm (>5wt.%) Pb while all other ablation spots for that sample gave <30 ppm. This indicates that inclusions can cause significant signal errors and calls all Pb concentration data into question, as any real lattice-bound Pb is likely to be 'swamped' by the inclusions causing skewing of the data. Most of the ablation spots across all analysed samples (Appendix A) gave relatively low lead readings, supporting the suggestion (Cook *et al.* 2009) that sphalerite is a poor host for lead due to ionic size differences between lead and zinc and that lead will most likely partition into galena where it is present.

Antimony was found at mostly above detection limits in all samples other than Mofjellet, ranging in abundance from below detection limits to 16 ppm except for Mt. Isa. Most values were between 0.1 and 4 ppm, with most ablation spots providing results below 1 ppm. The samples from Mt. Isa showed much higher antimony averages but these high mean values are heavily influenced by a small number of data points with anomalously high values.

Bismuth was found at mostly <mdl values for sample suites from Mofjellet, Bleikvassli and Broken Hill, but was above detection limits in Mt Isa, Røros and Sulitjelma. Bismuth was found to range from over >1 ppm to >500 ppm between ablation spots from sample STO-175-04 (from Røros), although many of the high bismuth values were found from ablation spots which also produced anomalously high lead and/or copper values. This suggests that many, or possibly all, of the high Bi readings resulted from inclusions of Cu-Pb-Bi sulphosalts within the sphalerite. From the other samples from Sulitjelma and Røros bismuth was found to be below 10 ppm except for one spot at Sulis 2b, which also produced an anomalously high copper value and so could have been inclusion related.

Elemental comparisons:

The results shown in Figure 10 show that there seems to be a positive correlation between In and Cu, Ag and Cu, and Ag and Pb. As Cu and Pb are considered to mostly exist within sphalerite as small inclusions, this link between these elements may indicate that Ag and In also exist primarily outside the sphalerite lattice proper. However, at least in the case of indium, previous studies (Cook *et al.* 2009; Cook *et al.* 2012) have invoked a coupled substitution between copper and indium ($2Zn^{2+} \leftrightarrow Cu^{+} + In^{3+}$) for In entering the sphalerite lattice, and as such the In could be lattice bound, in which case the presence of extensive chalcopyrite disease (See Figure 4 C and D for examples) introduces signal errors that could be masking a stronger correlation line. This study has found that samples from Mt. Isa, Røros, Sulitjelma and Bleikvassli are

seemingly enriched in Indium. This was not known at the time these deposits were under exploitation. In the case of Ag however, present literature (Cook *et al.* 2009) indicates where it is found in abundance it is usually found as microscopic Ag-bearing mineral inclusions in sphalerite. This indicates that the link between Ag and Cu, and between Ag and Pb, is most likely due to the same processes which affect the abundance of inclusions in sphalerite (mostly recrystallisation, possibly source rock and genetic type influence this too, too few deposits sampled to distinguish) result in the concentrations of all inclusion related elements being altered.

Figure 11 shows that there does not appear to be any universal trends linking manganese, iron and cadmium to each other. The Mn/Fe comparisons show no overall trend, which was not anticipated due to previous studies such as Di Benedetto *et al.* (2005) indicating that Mn and Fe compete in substituting for Zn in sphalerite, creating regions that are relatively high in one and low in the other which should result in a negative correlation between the two elements. As Di Benedetto *et al.* (2005) was focussed on studying sphalerite zonation, whereas the more general nature of this study involved ablation spots being taken towards the centre of sphalerite grains in order to minimise signal contamination from other grains the effects of zonation may have been masked in the results.

Effects of Metamorphism on sphalerite:

The broad effects of metamorphism and associated deformation on sulphide ores have been summarised in a number of publications (Vokes 1969; Mookherj 1970; Craig & Vokes 1993) . The effects on the distributions of minor and trace element distributions

are however less well constrained and there is little published data for sulphides other than pyrite.

As shown in Table 1, the six deposits from which the samples analysed in this study derive have all been regionally metamorphosed to some degree in their geological past. Together these six deposits cover a range of metamorphic grades from greenschist facies through lower and upper amphibolite facies up to granulite facies. From this the effects of metamorphism on the trace and minor elemental distributions of sphalerite can be analysed.

As shown by Table 2, both Mn and Ga do not appear to show any strong relationships to metamorphic grade or genetic type, apart from a possible positive correlation between average concentrations and metamorphic grade which, if it does exist at all is dwarfed by differences between individual samples from any given deposit. The range of concentrations at which they occur in the results are consistent values for VMS given in the literature (Cook *et al.* 2009 and references therein).

The ability for the Fe content of sphalerite to be used as a geobarometer has been well established in the literature for some time due to sphalerite-pyrite-pyrrhotite equilibrium resulting in sphalerite becoming progressively less Fe rich with increasing pressure (Scott and Barnes 1971; Scott 1973). However it has been shown that it cannot be used for geothermometry (Scott and Barnes 1971). No observable trend for Fe in relation to metamorphic grade can be found in the results, most likely due to the fact

that, in most cases, equilibrium crystallisation of sphalerite with both pyrite and pyrrhotite is lacking (Cook *et al.* 1994).

Cobalt was also found to have little correlation with metamorphic grade, the genetic type of the deposits seems to play a greater role than any subsequent metamorphism, with Røros, Sulitjelma (the two VMS deposits) and Broken Hill, which although it is classed as a SEDEX deposit has been noted to contain significant volcanic influences (Haydon & McConachy 1987) being the only deposits in which it was mostly found at concentrations above detection limits.

The effect of metamorphic grade on the heterogeneity of copper within the samples was quite distinctive, with the samples from the three highest grade deposits (Mofjellet, Bleikvassli and Broken Hill) showing significantly greater homogeneity in copper concentrations between ablation spots. An interesting point was that while the lower grade deposits showed greater mean copper concentrations overall, the means were affected by very high individual values. Most of the ablation spots being much lower in value, to the point where the median values for the three lowest grade deposits (Mt Isa, Røros and Sulitjelma) are within roughly the same order of magnitude as the copper concentrations of three highest grade ones. This indicates that without the effects of chalcopyrite disease on the copper concentration means, the average copper concentrations for the deposits are generally within a magnitude of each other. Sphalerite in sulphide deposits which have undergone high grade metamorphic recrystallisation having little to no chalcopyrite disease fits with the theory for how chalcopyrite disease originates given by Barton and Bethke (1987) in which a process of

replacement of high Fe sphalerite with an aggregate of chalcopyrite and low Fe sphalerite as a reaction occurring during cooling of the sphalerite, in that the high temperature recrystallisation of the higher grade deposits would result the reaction going the other direction and the chalcopyrite disease being absorbed back into the sphalerite. Equally, the relatively low grade metamorphism of Mt Isa, Røros and, to some extent Sulitjelma could possibly have resulted in more chalcopyrite disease through more low temperature reactions occurring.

While the average values for silver and cadmium show distinctive differences in range between the six deposits, no consistent trend in relation to metamorphic grade can be observed in the results.

Indium shows large variations in abundance both between deposits and between samples from the same deposits, as such no metamorphism related trend could be observed. Cook *et al.* (2009) considered that In enrichment in sphalerite is mostly linked to source rocks and the partitioning of the element among co-existing minerals. Lead shows even greater variance, with some ablation spots from the same sample sometimes differing in value by thousands of ppm, and as such similarly cannot be analysed for metamorphic influence.

Tin was found to occur at below detection limits in Mt Isa, Mofjellet and Broken Hill samples, and was only found at above detection limits in one sample from Sulitjelma. Due to large variations in abundance between samples from the deposits where it was found to be above detection limits, no trends can be observed.

Trace and minor elements in sphalerite

Antimony was found at mostly above detection limits in all samples except those from Mofjellet. However, due to high variance both between samples and between ablation spots from the same samples no clear trends could be observed from antimony.

Mercury was found at significantly above detection limits in all samples, allowing for any observable trends to be analysed. A possible trend of mercury being concentrated in upper amphibolite to lower granulite facies rocks (highest in Sulitjelma, Mofjellet and Bleikvassli) could exist, although a direct relation to increasing metamorphic grade is not supported since Broken Hill records the lowest mercury abundances on average.

Due to being found at mostly above minimum detection limits in only samples from Mt Isa, no metamorphic activity related trend could be observed for thallium. Concentrations of Tl may be influenced by the abundance of coexisting galena into which the element is preferentially partitioned at equilibrium conditions.

Bismuth was found to be mostly above minimum detection limits in samples from Mt Isa, Røros and Sulitjelma, which were the three lower metamorphic grade deposits and as such, a possible link between higher metamorphic grades resulting in lower bismuth concentrations in sphalerite. However, as Cook *et al.* (2009) mentions, bismuth is not considered to partition into sphalerite particularly well. The high standard deviations compared to means that the results for bismuth gave show that it is highly variable between ablation spots. This heterogeneity indicates that bismuth exists as small scale inclusions in sphalerite and as such the reduction at higher metamorphic grades could

simply be resulting from recrystallisation removing many of the smaller inclusions at higher grade.

It can be concluded that regional metamorphism will influence trace element concentrations to the extent that the distributions of some elements attain greater homogeneity in recrystallised sphalerite. The concentration ranges of the elements are however heavily influenced by the relative abundance of the elements in the pre metamorphic starting material, which in turn is controlled by the source rocks and the conditions at the time of initial crystallisation and on the partitioning of elements between sphalerite and other sulphides.

Possible future directions of study:

A key question raised by the results of this study is whether the sphalerite deposits analysed in this study are typical of sphalerite-bearing deposits in general. One way to confirm the results shown here would be to analyse a greater number of sphalerite-bearing deposits from different parts of the world, particularly MVT and skarn-related sphalerite, which were not sampled in this study. Such a continuation might attempt to assemble a collection of data encompassing a greater variety of locations, formation conditions and metamorphic histories. By adding the results of this and past studies a sizable body of data on the properties of natural sphalerite would be acquired, from which trends and correlations could be established and tested with greater confidence. Taking into consideration the importance of partitioning between coexisting minerals, future studies may wish to consider not just sphalerite, but also galena, chalcopyrite and other sulphides.

CONCLUSIONS:

. The large variability in apparent concentrations of Cu, Pb and Bi are most likely the result of non sphalerite sulphide grain inclusions within the sphalerite being tested. Where variability is lower for these elements (Bleikvassli, Broken Hill and Mofjellet) it is likely that the fewer inclusions have allowed for at some of the true lattice bound abundances to be shown. While the results are not conclusive as to Ag relationship to metamorphic grade, its correlation with Pb suggests Ag too may be an inclusion related element in sphalerite

. The mean concentrations of Cu, Pb and Bi appear to be reduced with increasing metamorphic grade, most likely due to a reduction in small scale inclusions.

. The genetic type of the sulphide deposit has a large influence over the cobalt content of the sphalerite. SEDEX type deposits contain little Co whereas VMS deposits have significant amounts.

ACKNOWLEDGEMENTS:

During the course of this study, I has benefitted from the instruments and training provided by Adelaide Microscopy, the convenient and helpful work environment and teaching provided by the University of Adelaide Geology and Geophysics department, advice and help given by Katie Howard and the extremely useful help and advice given by Associate Professor Nigel Cook, who supervised the production of this paper.

REFERENCES:

AXELSSON M. D. & RODUSHKIN I. 2001. Determination of major and trace elements in sphalerite using laser ablation double focusing sector field ICP-MS. *Journal of Geochemical Exploration* 72, 81-89.

BALABIN A. I. & URUSOV V. S. 1995. Recalibration of the sphalerite cosmobarometer - Experimental and theoretical treatment.*Geochimica Et Cosmochimica Acta* 59, 1401-1410.

BARRIE C. D., BOYLE A. P., COOK N. J. & PRIOR D. J. 2010a. Pyrite deformation textures in the massive sulfide ore deposits of the Norwegian Caledonides. *Tectonophysics* 483, 269- 286.

BARRIE C. D., COOK N. J. & BOYLE A. P. 2010b. Textural variation in the pyrite-rich ore deposits of the Roros district, Trondheim Region, Norway: implications for pyrite deformation mechanisms. *Mineralium Deposita* 45, 51-68.

BARTON P. B. & BETHKE P. M. 1987. Chalcopyrite disease in sphalerite - pathology and epidemiology. *American Mineralogist* 72, 451-467.

BINNS R. A. 1964. Zones of progressive regional metamorphism in the Willyama complex, Broken Hill district, New South Wales. *Journal of the Geological Society of Australia* 11, 283-330.

BJERKGARD T., MARKER M., SANDSTAD J.S., COOK N.J., SORDAHL T., 2001. Ore potential with emphasis on gold in the Mofjellet deposit, Rana, Nordland, Norway. *NGU* report 2001.050

CIOBANU C. L., COOK N. J., UTSUNOMIYA S., PRING A. & GREEN L. 2011. Focussed ion beam-transmission electron microscopy applications in ore mineralogy: Bridging micro- and nanoscale observations. *Ore Geology Reviews* 42, 6-31.

COOK N. J., HALLS C. & KASPERSEN P. O. 1990. The geology of the Sulitjelma ore field, northern Norway - some new interpretations.*Economic Geology and the Bulletin of the Society of Economic Geologists* 85, 1720-1737.

COOK N. J., HALLS C. & BOYLE A.P. 1993. Deformation and metamorphism of massive sulphides at Sulitjelma, Norway. *Mineralogical Magazine* 57, 67-81.

COOK N. J. 1993. Conditions of metamorphism estimated from alteration lithologies and ore at the Bleikvassli Zn–Pb–(Cu) deposit, Nordland, Norway. *Norsk Geologisk Tidsskrift* 73, 226– 233.

COOK N. J. 1994. Post-recrystallisation phenomena in metamorphosed stratabound sulphide ores: a comment. *Mineralogical Magazine* 58, 480-484.

COOK N. J. 1996. Mineralogy of the sulphide deposits at Sulitjelma, northern Norway. *Ore Geology Reviews* **11**, 303-338.

COOK N. J. 2001. Ore mineralogical investigation of the Mofjell deposit (Mo i Rana,Nordland, Norway) with emphasis on gold and silver distribution. *Norges geologiske undersøkelse* (NGU) Report 2001.051: 31 pp.

COOK N. J., CIOBANU C. L., PRING A., SKINNER W., SHIMIZU M., DANYUSHEVSKY L., SAINI-EIDUKAT B. & MELCHER F. 2009. Trace and minor elements in sphalerite: A LA-ICPMS study. *Geochimica Et Cosmochimica Acta* 73, 4761-4791.

COOK N. J., CIOBANU C. L., BRUGGER J., ETSCHMANN B., HOWARD D. L., DE JONGE M. D., RYAN C. & PATERSON D. 2012. Determination of the oxidation state of Cu in substituted Cu-In-Fe-bearing sphalerite via mu-XANES spectroscopy. *American Mineralogist* **97**, 476-479.

CORBETT G. J. & PHILLIPS G. N. 1981. Regional retrograde metamorphism of a high-grade terrain - the Willyama complex, Broken Hill, Australia. *Lithos* **14**, 59-73.

CRAIG J. R. & VOKES F. M. 1993. The metamorphism of pyrite and pyritic ores - an overview. *Mineralogical Magazine* **57**, 3-18.

DANYUSHEVSKY L., ROBINSON P., GILBERT S., NORMAN M., LARGE R., MCGOLDRICK P. & SHELLEY M. 2011. Routine quantitative multi-element analysis of sulphide minerals by laser ablation ICP-MS: Standard development and consideration of matrix effects. *Geochemistry-Exploration Environment Analysis* 11, 51-60.

DI BENEDETTO F., BERNARDINI G. P., COSTAGLIOLA P., PLANT D. & VAUGHAN D. J. 2005. Compositional zoning in sphalerite crystals. *American Mineralogist* 90, 1384-1392.

FROST B. R., MAVROGENES J. A. & TOMKINS A. G. 2002. Partial melting of sulfide ore deposits during medium- and high-grade metamorphism. *Canadian Mineralogist* **40**, 1-18.

FROST B. R., SWAPP S. M. & GREGORY R. W. 2005. Prolonged existence of sulfide melt in the Broken Hill orebody, New South Wales, Australia. *Canadian Mineralogist* **43**, 479-493.

FRYER B. J., JACKSON S. E. & LONGERICH H. P. 1995. Design, operation and role of the Laser-Ablation Microprobe coupled with an Inductively-Coupled Plasma - Mass-Spectrometer (LAM-ICP-MS) in the earth-sciences. *Canadian Mineralogist* 33, 303-312.

GRENNE T., IHLEN P. M. & VOKES F. M. 1999. Scandinavian Caledonide Metallogeny in a plate tectonic perspective. *Mineralium Deposita* 34, 422-471.

HAYDON R. C. & MCCONACHY G. W. 1987. The stratigraphic setting of Pb-Zn-Ag mineralization at Broken Hill. *Economic Geology* 82, 826-856.

JACKSON S. E., LONGERICH H. P., DUNNING G. R. & FRYER B. J. 1992. The application of Laser-Ablation Microprobe - Inductively Coupled Plasma-Mass- Spectrometry (LAM-ICP-MS) to insitu trace-element determinations in minerals. *Canadian Mineralogist* 30, 1049-1064.

KRAMER V., HIRTH H., HOFHERR W. & TRAH H. P. 1987. Phase studies in the systems Ag2Te-Ga2Te3, ZnSe-In2Se3, and ZnS-Ga2S3. *Thermochimica Acta* 112, 89-94.

LARGE R. R., BULL S. W., MCGOLDRICK P. J. & WALTERS S. 2005. Stratiform and Strata-Bound Zn-Pb-Ag Deposits in Proterozoic Sedimentary Basins, Northern Australia. *Economic geology and the bulletin of the Society of Economic* Geologists 100, 931-963

LEPETIT P., BENTE K., DOERING T. & LUCKHAUS S. 2003. Crystal chemistry of Fe-containing sphalerites. *Physics and Chemistry of Minerals* 30, 185-191.

LIN Y., COOK N. J., CIOBANU C. L., LIU Y., ZHANG Q., LIU T., GAO W., YANG Y. & DANYUSHEVSKIY L. 2011. Trace and minor elements in sphalerite from base metal deposits in South China: A LA-ICPMS study. *Ore Geology Reviews* 39, 188-217.

LOGAN M. A. 2004. Geochemistry of cadmium in sphalerite from Creede, CO, USA: A tool to study fractionation in hydrothermal systems. *Geochimica Et Cosmochimica Acta* 68, A77-A77.

MINCEVASTEFANOVA J. 1993. A morphological SEM study of wurtzite-sphalerite relationships in specimens from Zvezdel, Bulgaria. *Mineralogy and Petrology* 49, 119-126.

MORALEV G.V., LARSEN R.B. & BJERKGARD T. 1995. Distribution of precious metals in the Bleikvassli Zn-Pb SEDEX type deposit, Nordland, Norway. *NGU* report 95.154. Geological Survey of Norway.

MOOKHERJ.A 1970. Dykes, sulphide deposits, and regional metamorphism - criteria for determining their time relationship. *Mineralium Deposita* **5**, 120-&.

PAGE R. W. & SWEET I. P. 1998. Geochronology of basin phases in the western Mt Isa Inlier, and correlation with the McArthur Basin. *Australian Journal of Earth Sciences* 45, 219-232.

PATTRICK R. A. D., MOSSELMANS J. F. W. & CHARNOCK J. M. 1998. An x-ray absorption studyof doped sphalerites. *European Journal of Mineralogy* 10, 239-249.

PERKINS W. T., PEARCE N. J. G. & JEFFRIES T. E. 1993. Laser ablation inductively coupled plasma mass-spectrometry - a new technique for the determination of trace and ultra-trace elements in silicates. *Geochimica Et Cosmochimica Acta* 57, 475-482.

REED S. J. B. 1990. Recent deveolpments in geochemical microanalysis. *Chemical Geology* 83, 1-9.

ROSENBERG J. L., SPRY P. G., JACOBSON C. E., COOK N. J. & VOKES F. M. 1998.Thermobarometry of the Bleikvassli Zn-Ph-(Cu) deposit, Nordland, Norway. *Mineralium Deposita* 34, 19-34.

SCHWARTZ M. O. 2000. Cadmium in zinc deposits: Economic geology of a polluting element. *International Geology Review* 42, 445-469.

SCOTT S. D. 1973. Experimental calibration of sphalerite geobarometer.*Economic Geology* 68, 466-474.

SCOTT S. D. & BARNES H. L. 1971. Sphalerite geothermometry and geobarometry. *Economic Geology* 66, 653-669.

SOMBUTHAWEE C., BONSALL S. B. & HUMMEL F. A. 1978. Phase-equilibria in systems ZnS-MnS, ZnS-$CuLnS_2$, and MnS-$CuLnS_2$. *Journal of Solid State Chemistry* 25, 391-399.

SPRY P. G., PLIMER I. R. & TEALE G. S. 2008. Did the giant Broken Hill (Australia) Zn-Pb-Ag deposit melt? *Ore Geology Reviews* 34, 223-241.

SWAGER C. P. 1985. Cleavage and syntectonic vein development in the very low-grade dolomitic Urquhart Shale, Mount-Isa. *Journal of Structural Geology* 7, 499-499.

TAUSON V. L., CHERNYSHEV L. V. & MAKEEV A. B. 1977. Phase relations and structural peculiarities of mixed-crystals in ZnS-MnS system. *Geokhimiya*, 679-692.

Terramin Australia Limited 2012. Angas Geology and Mineralisation. *Terramin Australia*. Website last visited 15/05/2012, website address <http://www.terramin.com.au/projects/angas/geology.aspx>

VAUGHAN D. J. & CRAIG J. R. 1978. The mineral chemistry of metal sulfides. Cambridge University Press, Cambridge, London, New York and Melbourne, 493p.

VOKES F. M. 1969. A review of metamorphism of sulphide deposits. *Earth-Science Reviews* **5**, 99-&.

WATLING R. J., HERBERT H. K. & ABELL I. D. 1995. The application of laser ablation inductively coupled plasma mass spectrometry (LA-ICP-MS) to the analysis of selected sulfide minerals. *Chemical Geology* 124, 67-81.

WILSON S. A., RIDLEY W. I. & KOENIG A. E. 2002. Development of sulfide calibration standards for the laser ablation inductively-coupled plasma mass spectrometry technique. *Journal of Analytical Atomic Spectrometry* 17, 406-409.

YE L., COOK N. J., LIU T. G., CIOBANU C. L., GAO W. & YANG Y. L. 2012. The Niujiaotang Cd-rich zinc deposit, Duyun, Guizhou province, southwest China: ore genesis and mechanisms of cadmium concentration. *Mineralium Deposita* 47, 683-700.